J. Fluid Mech. (1989), *vol.* 206, *pp.* 223–263
Printed in Great Britain

The influence of initial deformation on drop breakup in subcritical time-dependent flows at low Reynolds numbers

By H. A. STONE[1] AND L. G. LEAL[2]

[1] Division of Applied Sciences, Harvard University, Cambridge, MA 02138, USA

[2] Department of Chemical Engineering, California Institute of Technology, Pasadena, CA 91125, USA

(Received 28 June 1988 and in revised form 25 January 1989)

Transient effects associated with the deformation and breakup of a drop following a step change from critical to subcritical flow conditions are studied experimentally and numerically. In the experiments, we consider step changes in both the shear rate and flow type for two-dimensional linear flows generated in a four-roll mill. Numerically we consider step changes in shear rate only for a uniaxial extensional flow. Depending upon the degree of deformation prior to the change in flow conditions, the drop may either return to a steady deformed shape, or continue to stretch at a reduced rate, or, for intermediate cases, the drop may break without large-scale stretching. This behaviour is a consequence of the complicated interaction between changes of shape due to interfacial tension and changes of shape due to the motion of the suspending fluid. This mode of breakup is most pronounced for high viscosity ratios, because very large extensions are necessary to guarantee breakup if the flow is stopped abruptly. For drops that are not too deformed, the sudden addition of vorticity to the external flow is characterized by rapid rotation of the drop to a new steady orientation followed by deformation and/or breakup according to the effective flow conditions at the new orientation. Finally, for viscous drops in flows with vorticity, it is demonstrated experimentally that breakup can be achieved if the initial shape is sufficiently non-spherical even though the same drop could not be made to break in the same flow at any capillary number when beginning with a near-spherical shape.

1. Introduction

G. I. Taylor's investigation of the deformation and breakup of liquid droplets (1932, 1934) were motivated by an interest in emulsion formation and mixing processes. In recent years the areas of application have widened and drop deformation studies have found use in characterizing the flow-induced deformation of flexible bodies, e.g. cells, as well as certain material science problems (Seward 1974). However, time-dependent deformation associated with the actual fragmentation of the droplet and how this is related to breakup in the presence of time-dependent flows has not been carefully studied. An introduction to some qualitative features associated with drop breakup in transient flows is presented in this paper.

The majority of analytical, experimental and numerical studies of drop deformation and breakup at low Reynolds numbers have considered the case of a single drop suspended in a steady linear flow field with particular atttention given to

predicting the steady drop shapes and orientations that result from a balance of viscous and interfacial forces. Two excellent review articles concerning much of the work prior to 1983 have been written by Acrivos (1983) and Rallison (1984). In these flows the non-existence of a steady-state shape results in a continuous stretching motion of the droplet. In spite of the fact that this continuous stretching is called 'break-up' and is characterized by a critical value of the capillary number (dimensionless shear rate), complete facturing of droplets in steady linear flows has been reported by Mikami, Cox and Mason (1975) only for the case of extremely elongated, cylindrical droplets that break due to capillary instabilities.

The only extensive experimental study of transient effects has been reported by Grace (1971) who considered both simple shear and planar extensional flows, and documented a number of fascinating phenomena, including the effect of abruptly stopping the flow (first observed by Taylor 1934), the use of a programmed gradual reduction of the shear rate to produce breakup without gross stretching of the drop, and a systematic study of the number of drop fragments produced when breakup occurs at a shear rate that exceeds the critical value. Additional transient experiments are described by Torza, Cox & Mason (1972) who report that the mechanism for breakup may depend on the rate at which the shear rate is increased. In a numerical study that is concerned primarily with calculating steady drop shapes, Rallison & Acrivos (1978) discuss observations concerned with breakup due to the application of a subcritical flow to a drop originally stretched by a stronger flow.

It is clear from the above studies that transient flows play an important role in the breakup process, though many qualitative and quantitative questions remain. For example: What is the effect of non-spherical initial shape on the capillary number necessary to guarantee that the drop does not return to a steady shape? How does the drop shape evolve and what is the mode of fragmentation? What is the effect of viscosity ratio? In order to answer some of these questions, we have initiated a combined experimental and numerical study of the time-dependent dynamics of drop deformation and breakup. In the first part of our investigation (Stone, Bentley & Leal 1986), we experimentally examined the time-dependent stretching of a drop in steady flows at the critical capillary number, as well as the interfacial-tension-driven relaxation and breakup processes that result when the flow is stopped abruptly with the drop in an elongated state. In no case did we observe actual fragmentation while the flow was maintained. Further, the breakup process that occurred for a sufficiently elongated drop when the flow was stopped was not a capillary-wave instability, but consisted of the formation and breakoff of bulbuous ends of the drop via a deterministic process we described as 'end-pinching'. The second part of our study (Stone & Leal 1989) made use of the boundary-integral method to probe numerically this time-dependent breakup phenomena and clearly exposed the mechanism for breakup, in addition to explaining the dependence of the pinch-off process on viscosity ratio. The experimentally observed drop dynamics were reproduced completely with the assumption of a constant interfacial tension. In addition, the numerical method was used to explore the effect of including finite-amplitude capillary waves on the initial drop shape. These studies, including numerically generated velocity fields inside and outside the drop, provide an improved understanding of the mechanisms of drop breakup due to interfacial-tension-driven motions in an otherwise quiescent fluid. However, this is only a first step in understanding more complicated time-dependent flows.

The novel flow situation examined in this paper is the behaviour of a modestly

deformed drop in a subcritical time-dependent flow. The term 'modestly deformed' refers to a shape that is more deformed than the maximum steady shape, but is not highly elongated. We focus experimentally on step changes from the critical capillary number (where the drop is slowly extending) to subcritical (weaker) flow conditions, either by decreasing the shear rate or by suddenly adding vorticity to the flow. The addition of vorticity indirectly decreases the effective shear rate experienced by the drop by rotating the drop away from the principal axis of strain of the undisturbed flow field. Thus, the effective shear rate (i.e. the local rate of stretching of a fluid element orientated in the direction of maximum droplet elongation) is reduced (Bentley & Leal 1986*b*) and, as a consequence, the effective capillary number is reduced. The application of a (weak) straining motion to a drop originally stretched by a stronger flow involves an interaction between an interfacial-tension-driven flow tending to cause relaxation of the drop to a less deformed shape, and the (subcritical) extensional flow that tries to continue to elongate the drop. We provide several examples of complete breakup in such flows. The boundary-integral method is used to extend these experimental observations by probing the details of the flow field both external and internal to the drop.

It should be added that dynamics associated with transient deformation of a bubble in axisymmetric extensional flows at finite Reynolds numbers have been described recently by Kang & Leal (1987) and aspects of the behaviour detailed in their study are analogous to observations reported here. There are also a number of quite varied processes where interfacial-tension-driven motions similar to those illustrated in this paper play an important role. For example, Lasheras, Fernandez-Pello & Dryer (1979) have observed breakup of stretched liquid droplets in an experimental study of the combination of fuel droplets, and transient effects similar to those discussed here may be expected in electrohydrodynamic or magneto-hydrodynamic breakup of droplets (e.g. see Torza, Cox & Mason 1971 and Sherwood 1988) if the field producing the deformation is time-dependent.

2. Problem statement

In this paper, we report on a combined experimental and numerical investigation of drop deformation and breakup in time-dependent extensional flows. To facilitate the discussion, it is convenient to discuss the common conditions of experiment and theory, and to introduce some basic nomenclature.

Thus, we consider a neutrally buoyant Newtonian liquid drop with undeformed radius, a and viscosity $\hat{\mu}$ suspended in a second immiscible Newtonian fluid with viscosity μ. The viscosity ratio is denoted as $\lambda = \hat{\mu}/\mu$. Previous comparisons of experimental and theoretical results have demonstrated that the interface for the systems studied experimentally can be characterized completely by a constant interfacial tension σ. In addition, the drop Reynolds numbers (based on μ) for the experiments were $O(10^{-4})$ or smaller, and the numerical work is thus based upon the creeping flow approximation. Far from the drop, the undisturbed flow in the theory is assumed to vary linearly with position.

$$\boldsymbol{u}_\infty = \boldsymbol{\Gamma}(t)\cdot\boldsymbol{x} \tag{1}$$

where $\boldsymbol{\Gamma}(t)$ is the velocity gradient tensor, which may depend on time. In the experiments, which are carried out in a four-roll mill, the lengthscale characteristic of the drop is much smaller than the distance over which significant velocity gradient variations occur, and thus the flow is also closely approximated by the form (1).

For the same reason, a linear approximation of the base flow is also relevant in many applications. For the numerical work, we examine the particular case of axisymmetric extensional flow where $\boldsymbol{\Gamma}$ is diagonal,

$$\boldsymbol{\Gamma}(t) = \tfrac{1}{2}G(t)\begin{pmatrix} -1 & 0 & 0 \\ 0 & -1 & 0 \\ 0 & 0 & 2 \end{pmatrix}. \tag{2}$$

Experimentally, we study two-dimensional linear flows where $\boldsymbol{\Gamma}$ has the form

$$\boldsymbol{\Gamma}(t) = \tfrac{1}{2}G(t)\begin{pmatrix} 1+a(t) & 1-a(t) & 0 \\ -1+\alpha(t) & -1-\alpha(t) & 0 \\ 0 & 0 & 0 \end{pmatrix}. \tag{3}$$

The shear rate G represents the magnitude of $\boldsymbol{\Gamma}$ and α is a flow-type parameter that provides a measure of the ratio of the rate of strain to the vorticity. Typical streamlines for different choices of α have been sketched in previous publications from our laboratory (e.g. Bentley & Leal 1986*b*). We note that the ratio of the vorticity and strain rate of the undisturbed two-dimensional flow is equal to $(1-\alpha)/(1+\alpha)$, so that $\alpha = 1.0$ corresponds to two-dimensional extensional flow and $\alpha = 0$ corresponds to simple shear flow. Viscous stresses generated at the droplet surface cause deformation that is resisted by interfacial tension. The relative importance of viscous and interfacial tension forces is measured by the capillary number, $\mathbb{C} = \bar{G}\mu a/\sigma$, where $\bar{G}$ indicates a representative value of the time-dependent shear rate.

It is convenient to characterize the degree of deformation using a single scalar parameter. For this study, we shall consider drops that are significantly deformed and in these instances it is appropriate to use a dimensionless extension ratio, L/a, where $2L$ is the end-to-end drop length.

The great majority of studies in the low-Reynolds-number drop deformation literature have focused on the steady-state effects of $\mathbb{C}$, λ, and the tensorial character of $\boldsymbol{\Gamma}$. Our present concern is time-dependent behaviour. In this case, as outlined by Rallison (1984), two additional parameters are introduced: the initial shape of the drop and the history of the flow as specified by $\boldsymbol{\Gamma}(t)$.

The objective of the present work is to understand drop deformation and breakup in flows where a sudden change in either the flow strength or the flow type occurs. The experimental part of the investigation focuses on step changes in shear rate and/or flow type for two-dimensional flows generated in a four-roll mill. Complementing the experiments, the boundary-integral method is then used to study step changes in shear rate for axisymmetric extensional flows, and illustrates the external and internal velocity fields together with the interface evolution. Specifically, we examine the effect of initial deformation of the drop on the capillary number needed to produce breakup, the effect of vorticity of the imposed flow and the role played by the viscosity ratio.

3. The experiment

Experimentally, we study drop dynamics in two-dimensional flows generated in a computer-controlled four-roll mill. The application and use of this device have been documented in three previous publications from our laboratory (Bentley & Leal 1986*a*, *b*; Stone *et al.* 1986). To summarize briefly, the four-roll mill consists of four

cylindrical rollers, placed at the corners of a square, which are rotated to create an approximation to a two-dimensional linear flow field in the region between the rollers. A drop is placed at the central stagnation point of the flow. Because the drop position at the stagnation point is unstable, a control scheme is used to regulate the roller speeds in a manner that keeps the drop position fixed while maintaining the shear rate and flow type at specified values. This control algorithm has proven very effective and we have demonstrated that the small roller speed changes that occur produce no observable drop deformation (Stone *et al.* 1986). Hence, we believe that the transient effects seen in this study are strictly due to the programmed changes in flow conditions.

The experimental parameters are such that changes in flow conditions, manifested by changes in roller speeds and vorticity diffusion into the fluid, occur on a timescale $\lesssim 0.3$ s, which is relatively fast compared with the time, typically $\gtrsim 1$ s, for significant drop deformation to occur (Stone *et al.* 1986). Therefore, a good approximation to step changes in flow conditions is produced by abrupt changes in roller speeds and we shall refer to the transients as 'step changes in the flow'.

The experimental procedure we have followed is to increase the shear rate in small increments so that the drop progresses through a series of steady states. When the critical shear rate, characterized by non-existence of a steady shape, is reached, the droplet slowly extends. At some point, conveniently represented by the instantaneous elongation ratio, L/a, the flow conditions are altered abruptly to subcritical or weaker flow conditions. In other words, the shear rate will either be decreased or the new flow conditions will have a higher vorticity-to-strain-rate ratio (smaller α). In addition, a small number of experiments will be described where simultaneous step changes in shear rate and flow type occur. It is only in these subcritical flow situations that it is not possible *a priori* to 'guess' the consequence of the flow change. However, a few experiments and numerical simulations were performed that examined step changes from a critical capillary number to supercritical capillary numbers. In all cases, the drop was rapidly stretched without breaking to the limit of the linear flow region of the four-roll mill. In these supercritical flows, the most significant observation was that the ends were not as bulbous as when the drop was stretched at the critical shear rate, and the midsection remained cylindrical.

For the reader's reference, the undeformed drop radii are $a \approx 0.1$ cm, the suspending fluid has a viscosity $\mu \approx 50$ g/cm s^{-1} and a density $\rho \approx 1$ g/cm^3, and the interfacial tensions for the fluid–fluid systems used are $\sigma \approx 5$ dynes/cm. The shear rates necessary to produce breakup vary with viscosity ratio and flow type (α) but are generally in the range 0.1–0.3 s^{-1} so that $0.1 < \mathbb{C} < 0.3$. The corresponding Reynolds numbers, $\rho\sigma a/\mu^2$ and $\rho\bar{G}a^2/\mu$, are typically $O(10^{-4})$. The experiments reported here cover the range $0.2 \leqslant \alpha \leqslant 1.0$ and $0.01 \leqslant \lambda \leqslant 20$.

4 Experimental results: step changes in shear rate

4.1. *Two-dimensional straining flows, $\alpha = 1.0$*

Let us begin the discussion of experimental results by examining the effect of a step change in shear rate for a modestly extended drop, the flow type being maintained constant. Figure 1 illustrates an abrupt reduction from the critical capillary number $\mathbb{C}_c$† to $\mathbb{C} = 0.5\mathbb{C}_c$ at three different initial extensions for $\lambda = 0.1$ and $\alpha = 1.0$ (a two-

† We denote the limiting capillary number for non-existence of a steady drop shape in a steady flow as the critical capillary number, $\mathbb{C}_c$.

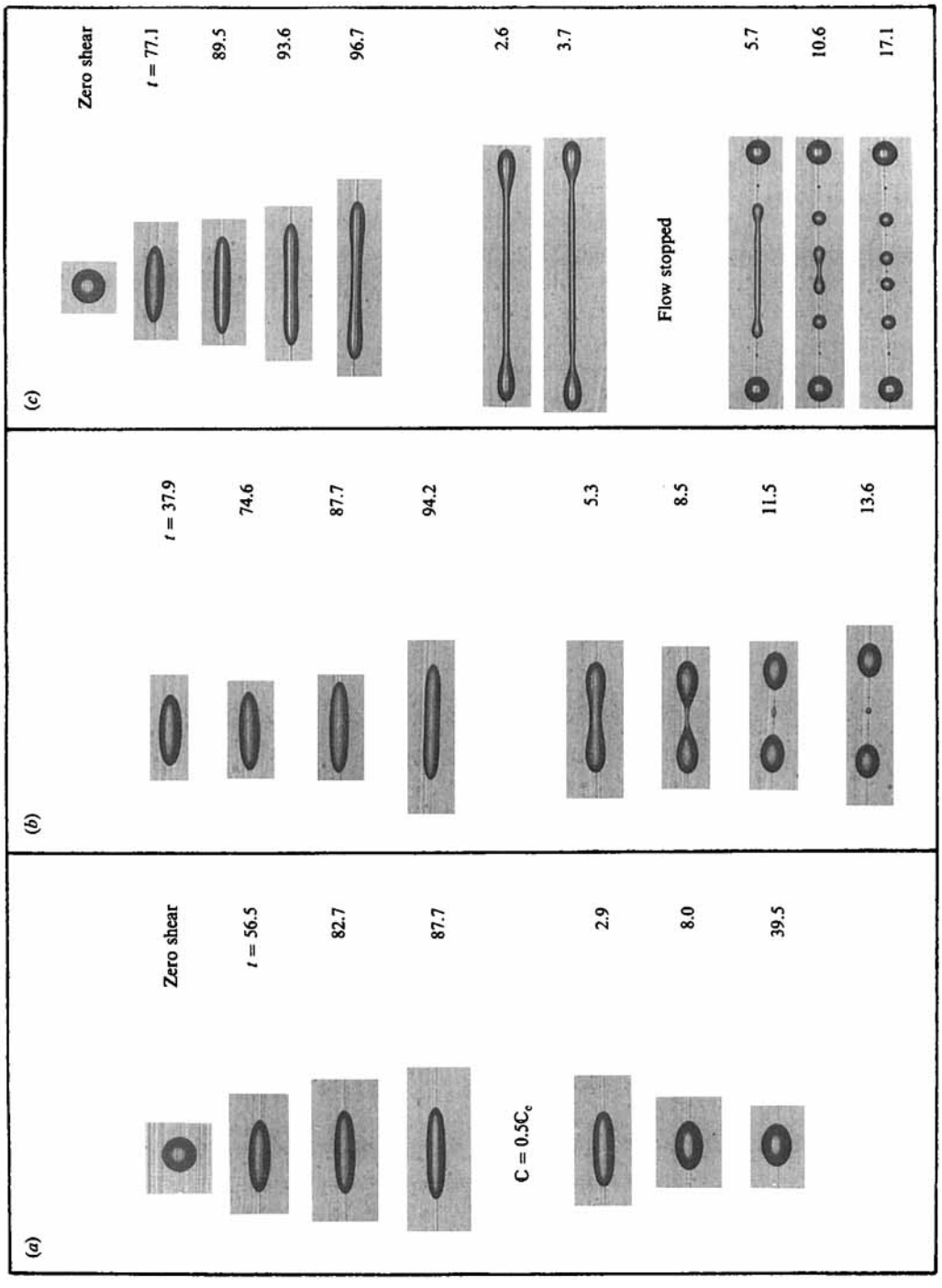

FIGURE 1. The effect of a step reduction in shear rate; the flow type is maintained constant. $\lambda = 0.1$; $a = 1.0$. Step change from $\mathbb{C}_c$ to $0.5\mathbb{C}_c$; $\mathbb{C}_c = 0.174$.

dimensional extensional flow for which $\mathbb{C}_c = 0.174$). A photograph of the undeformed droplet is shown for reference. Dimensionless time is shown to the right of each photograph, non-dimensionalized with respect to the interfacial tension timescale $t_c = a\mu/\sigma$.‡ This timescale is convenient for comparison of studies at different viscosity ratios since it remains unchanged as λ varies. For parameters typical of the experiments reported in this paper $t_c \approx 1$ s. Whenever a step change in the velocity field occurs, time is measured with respect to the instant the change is made. In each of the figures the first few photographs show the droplet extending in a steady flow at the critical capillary number. The droplet shape during this elongation process consists of a cylindrical midsection with rounded ends. Then, the shear rate is reduced abruptly, as described above.

In figure 1 (*a*) the subcritical shear rate $0.5\mathbb{C}_c$ is not sufficient to cause breakup for the degree of extension shown. In particular, interfacial tension dominates and drives the drop back to a steady shape. So far as we can discern from still photographs of the cross-sectional shape of the drop, the new steady shape is precisely the same as would be achieved by applying the reduced capillary number, $\mathbb{C} = 0.5\mathbb{C}_c$, to an initially spherical drop. This is true in general. In all experiments conducted, for $0.2 < \alpha < 1.0$ and $0.01 < \lambda < 20$ and a wide range of shear rate and flow type changes, whenever a steady drop shape is achieved, it is the same as found in the steady-state experiments with the same final flow conditions, and a spherical initial shape.

In figure 1 (*b*) the drop is slightly more elongated prior to the abrupt change from $\mathbb{C}_c$ to $0.5\mathbb{C}_c$ and drop breakup occurs in the flow. Two large daughter droplets are formed with a small satellite drop visible in between. The small satellite drop forms from the fluid cylinder that connects the two large bulbous ends just prior to breakup. It was observed in our previous experiments that breakup via interfacial-tension-driven motion in the absence of an external flow occurs only if the initial shape is quite elongated. Further, in the presence of a steady motion with $\mathbb{C} = \mathbb{C}_c$, the drop extends continuously, but is not observed to break even when quite extreme elongations are produced. Here, however, drop breakup occurs in a flow without large-scale stretching of the droplet.

Finally, figure 1 (*c*) shows how the two competing flow mechanisms, associated with interfacial tension and the external flow, interact for a more highly stretched droplet. Shortly after the abrupt change in flow, the droplet begins to stretch at a rate similar to a line element of the fluid, but the ends are continually bulbing and the development of a pinching region near the bulbous ends is evident. This pinching would presumably lead eventually to droplet breakup if the flow field was maintained, but, in the case shown here, the experiment was stopped prior to this as the ends of the droplet approached the limits of the linear flow region of the four-roll mill. For clarity, it is convenient to distinguish this stretching process (which presumably leads to breakup via pinch-off of the ends) from the complete breakup in the absence of stretching that is illustrated in figure 1 (*b*). Thus, in the remainder of this paper, whenever a subcritical flow causes the droplet to stretch but does not produce complete fragmentation during the time the drop remains within the linear flow region of the four-roll mill, we shall use the terminology 'breakup via continuous stretching'. After the flow is stopped in figure 1 (*c*), the droplet fragments according to the basic end-pinching mechanism. This aspect of the breakup dynamics, due to

‡ As discussed by Stone *et al.* (1986), the zero of time is subject to some error due to the small experimental uncertainty in determining the critical capillary number coupled with the very slow elongation process that accompanies stretching at $\mathbb{C}_c$.

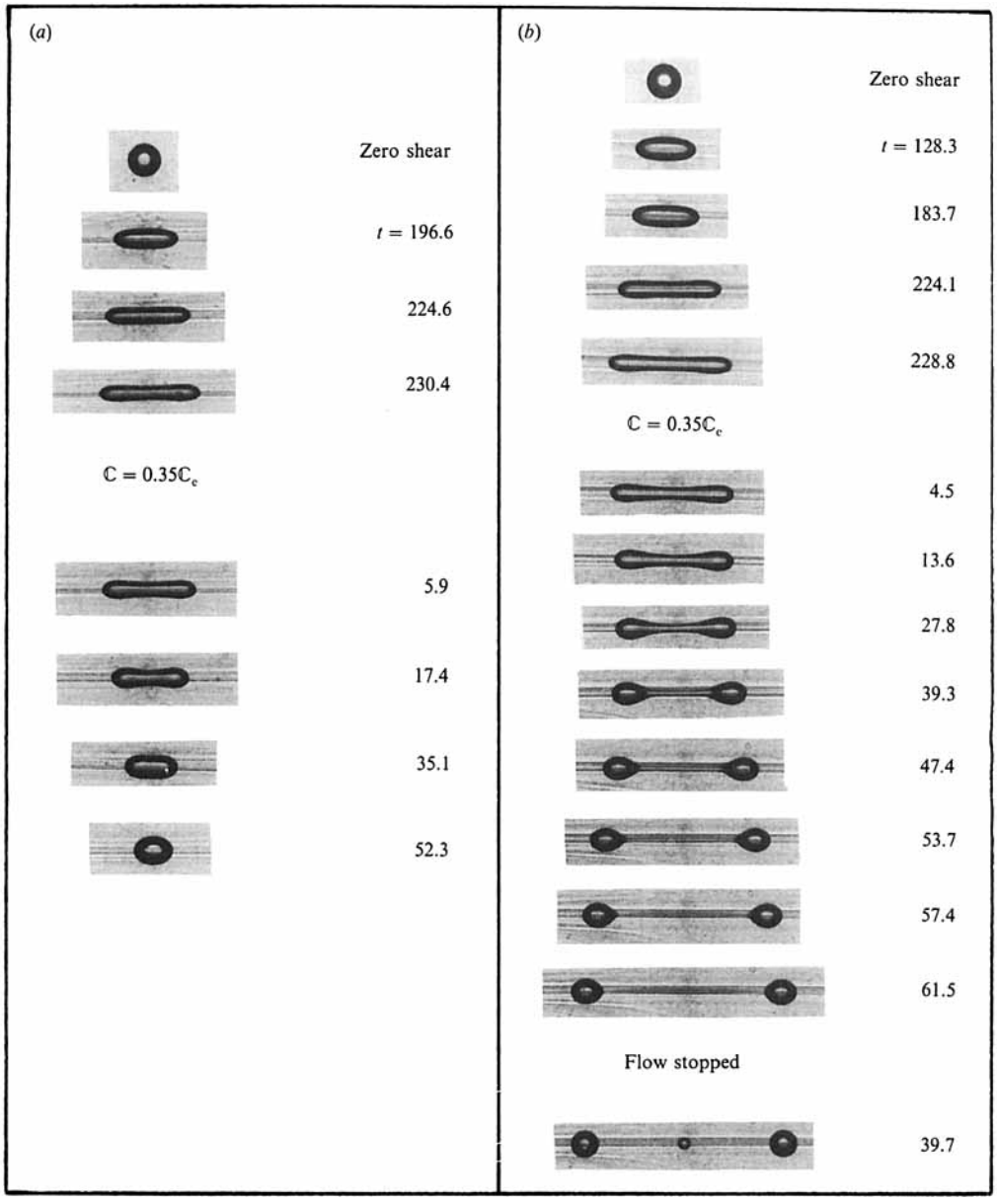

FIGURE 2. The effect of a step reduction in shear rate; the flow type is maintained constant. $\lambda = 5.1$; $\alpha = 1.0$. Step change from $\mathbb{C}_c$ to $0.35\mathbb{C}_c$, $\mathbb{C}_c = 0.12$.

an interfacial tension-driven flow produced by curvature variations along the drop surface, has been discussed experimentally and numerically in two previous papers from our laboratory (Stone *et al.* 1986 and Stone & Leal 1989).

A second example of the relaxation and breakup process following a step change in shear rate is shown in figure 2 for a larger viscosity ratio, $\lambda = 5.1$, and a larger change in shear rate from $\mathbb{C}_c$ down to $0.35\mathbb{C}_c$. Figure 2(*a*) illustrates a case in which the drop relaxes back to a steady shape even though intermediate shapes exhibit a pronounced formation of a neck in the middle of the drop that is very reminiscent

of figure 1(*b*). The main difference in this case is that the drop simultaneously shortens to a greater extent than in figure 1(*b*) owing to the weaker applied flow, and eventually returns to a steady shape. Figure 2(*b*) shows a case in which the viscous drop is somewhat more extended initially. Clearly, the drop breaks in a manner resembling figure 1(*b*, *c*), but there is an extended period after the reduction in shear rate where the drop shortens and is maintained in 'dogbone-like' shape before it finally begins to stretch and develop a pinch near the bulbous end that leads to breakup, as shown in the last few photographs. With the larger value of λ and the weaker flow after the step change, the complete breakup mode without stretching, seen in figure 1(*b*), was never observed in the present experiments.

The photographs in figures 1 and 2 demonstrate a number of features common to all of the step-change experiments we have conducted. Depending upon the value of L/a at the moment of the step reduction in shear rate, and the magnitude of the jump, one of three things may occur. First, below a certain critical value of L/a and/or β (where the capillary number after the jump is denoted as $\beta\mathbb{C}_c$), the drop shortens and returns to an equilibrium steady shape. Second, if β and/or L/a is increased somewhat, the drop may first shorten and develop bulbous ends, but then breaks via 'end-pinching' with little stretching prior to breakup. Finally, with larger values still for β and/or L/a, the drop just continues to stretch at a rate set by the new flow conditions and the development of a pinching region, though often observed, may not be sufficient to cause breakup within the linear flow region of the apparatus.

Initially one might think that the 'dogbone' conformations, which sometimes exist for extended periods of time, may be steady shapes that break because they are unstable with respect to small disturbances in the flow (due, for example, to the action of the control algorithm). However, the reproducible nature of the phenomena in many experiments and numerical simulations (to be illustrated in many figures in this paper) suggest that this is not the case. Rather, the complicated dynamics simply evolve on a long timescale. These dynamics are a consequence of the interaction of the extensional character of the flow, which drains fluid from the central cylindrical region while also trying to further stretch the droplet, and an interfacial-tension-driven motion, which causes bulbing of the ends and a relaxational motion that is reminiscent of the end-pinching phenomenon. Detailed velocity fields that illustrate the shape evolution will be presented in the numerical study described in §8.

4.2. *Flows with vorticity*, $\alpha \neq 1.0$

One question which comes to mind at this point concerns the effect of flow type. How are the previously illustrated dynamics affected if $\alpha \neq 1$? To answer this question, we carried out step-change experiments for a number of fixed values of $\alpha \neq 1$. To understand the results, it is useful to review the role of flow type in the steady-state experiments of Bentley & Leal (1986*b*), and in the transient experiments of Stone *et al.* (1986). First, in steady flows at subcritical capillary numbers, drops initially deform along the principle axis of strain for all α, but for $\alpha \neq 1$, as the capillary number is increased, drops gradually reorientate until at $\mathbb{C} \sim \mathbb{C}_c$, the drop axis is aligned along the outflow axis† of the linear flow field. At this orientation the drop experiences an effective shear rate $G_c \alpha^{\frac{1}{2}}$ (G_c is the shear rate at the critical capillary number). Thus, for transient stretching at $\mathbb{C} \sim \mathbb{C}_c$, the drop stretches along the axis at a rate proportional to $(G_c \alpha^{\frac{1}{2}})^{-1}$, but the stretching process and the drop shape are

† The outflow axis is the direction defined by the eigenvector of equation (3) with eigenvalue $+\alpha^{\frac{1}{2}}$.

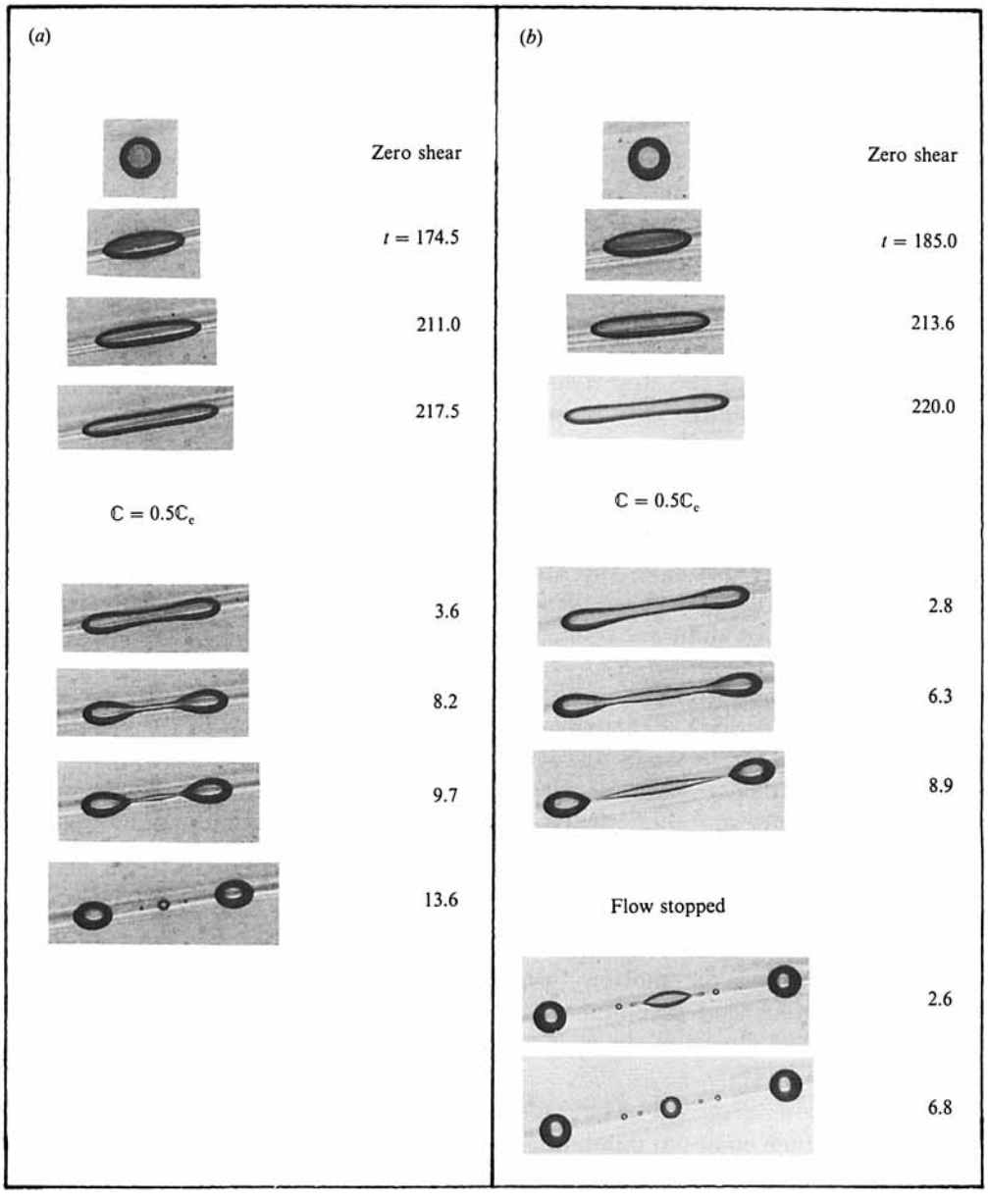

FIGURE 3. The effect of a step reduction in shear rate; the flow type is maintained constant. $\lambda = 0.1$; $\alpha = 0.6$. Step change from $\mathbb{C}_c$ to $0.5\mathbb{C}_c$; $\mathbb{C}_c = 0.23$.

otherwise largely unaffected by the flow type for $0.2 \leqslant \alpha \leqslant 1$. In view of these results, it is clear that the influence of flow type in the present step change in shear rate experiments (for fixed $\alpha \neq 1$) must depend on whether a stretched drop remains oriented along the outflow axis when the magnitude of the velocity gradient is reduced suddenly.

In order to illustrate the effect of flow type, figure 3 presents a step change in shear rate for $\lambda = 0.1$ and a flow type $\alpha = 0.6$. The step change in this case corresponds to a decrease from a critical capillary number, $\mathbb{C}_c = 0.23$ for this value of α, to

$\mathbb{C} = 0.5\mathbb{C}_c$. Clearly, the dynamics are very similar to those shown in figures 1 and 2. After the decrease in capillary number, the drop remains oriented in the direction of the outflow axis even though the same drop, with a steady-state ellipsoidal shape appropriate to these conditions ($\mathbb{C} = 0.5\mathbb{C}_c$), would have an orientation between the principal axis of strain (the horizontal direction) and the outflow axis. In figure 3, the more elongated initial shape is responsible for the fact that the drop remains oriented along the outflow axis even in subcritical flow conditions.

Figures 1 and 3 correspond to the same value of $\lambda = 0.1$, and thus provide a direct visual comparison of the effect of flow type for a step reduction in shear rate. The qualitative similarity evident in the relaxation and breakup process is clear. In addition, a series of experiments, including those displayed in figures 1 and 3, was carried out to determine the critical initial elongation needed for breakup at $\lambda = 0.1$ given a reduction to $\mathbb{C} = 0.5\mathbb{C}_c$. For the $\alpha = 1.0$ flow, the critical elongation is bounded by $3.0 < L/a < 3.2$, while for the $\alpha = 0.6$ flow the critical elongation is bounded by $3.0 < L/a < 3.3$. In fact, for a fixed value of λ, the critical elongation for breakup in a step to $\mathbb{C} = \beta\mathbb{C}_c$ was found to depend only on β and not on the flow-type parameter α for $\alpha > 0$. Clearly, small detailed changes occur in the shape as the flow type varies. Therefore, as a result of the qualitative and quantitative agreement observed above, we conclude that the response to a step change in shear rate depends primarily on the global features of the drop shape rather than on any local details. A similar conclusion was reached in the end-pinching studies of Stone *et al.* (1985).

Two additional examples of the effect of a step change in shear rate which further corroborate the invariance to flow type are shown in figures 4 and 5 for $\lambda = 1.3$ and $\lambda = 5.3$, respectively. Figure 4(*a*) shows a step reduction to $\mathbb{C} = 0.75\mathbb{C}_c$ for a flow type $\alpha = 0.2$ and figure 4(*b*) shows the same step reduction for an $\alpha = 0.6$ flow. Again we observe relaxation back to a steady shape if the droplet is not too elongated and breakup via continuous stretching if the step change occurs with the droplet more elongated. In figure 5, step-reduction experiments are shown for $\mathbb{C} = 0.5\mathbb{C}_c$ and a flow type $\alpha = 0.4$. The experiment illustrated in figure 5(*b*) is well documented and shows complete fracturing into two large droplets with a thin thread in between. The initial response to the abrupt step change is a reduction in end-to-end length, bulbing of the ends, and then a gradual thinning of the droplet midsection with almost no change in overall length. Finally, the droplet stretches, the middle region is drawn into a very thin cylinder and a pinch process occurs near the ends. The final photograph shows the final stage of fragmentation. After the flow is stopped, the central thin thread, which has pointed ends, returns to a single droplet.

The qualitative features illustrated by figures 3–5 are the same as those outlined in figures 1 and 2. Furthermore, even after the step change in shear rate, the elongated droplet maintains an orientation along the exit streamline (the effective shear rate for a fluid element at this orientation is $G\alpha^{\frac{1}{2}}$) and this is true even for initial L/a values where the drop eventually relaxes back to an equilibrium shape. In those cases where a steady ellipsoidal shape is finally established, the drop relaxes back almost to the steady shape prior to rotating away from the outflow axis towards the final orientation. As a result of these observations, we may conclude that for changes in shear rate only, the primary independent effect of flow type is to determine the critical capillary number and the proper timescale of the subsequent relaxation or stretching and breakup processes.

It is informative to study the relaxation and stretching processes illustrated above by displaying the dimensionless drop length as a function of time. In figure 6(*a*, *b*), typical data for L/a versus time are shown for the cases $\lambda = 0.1$ and 5.3, respectively.

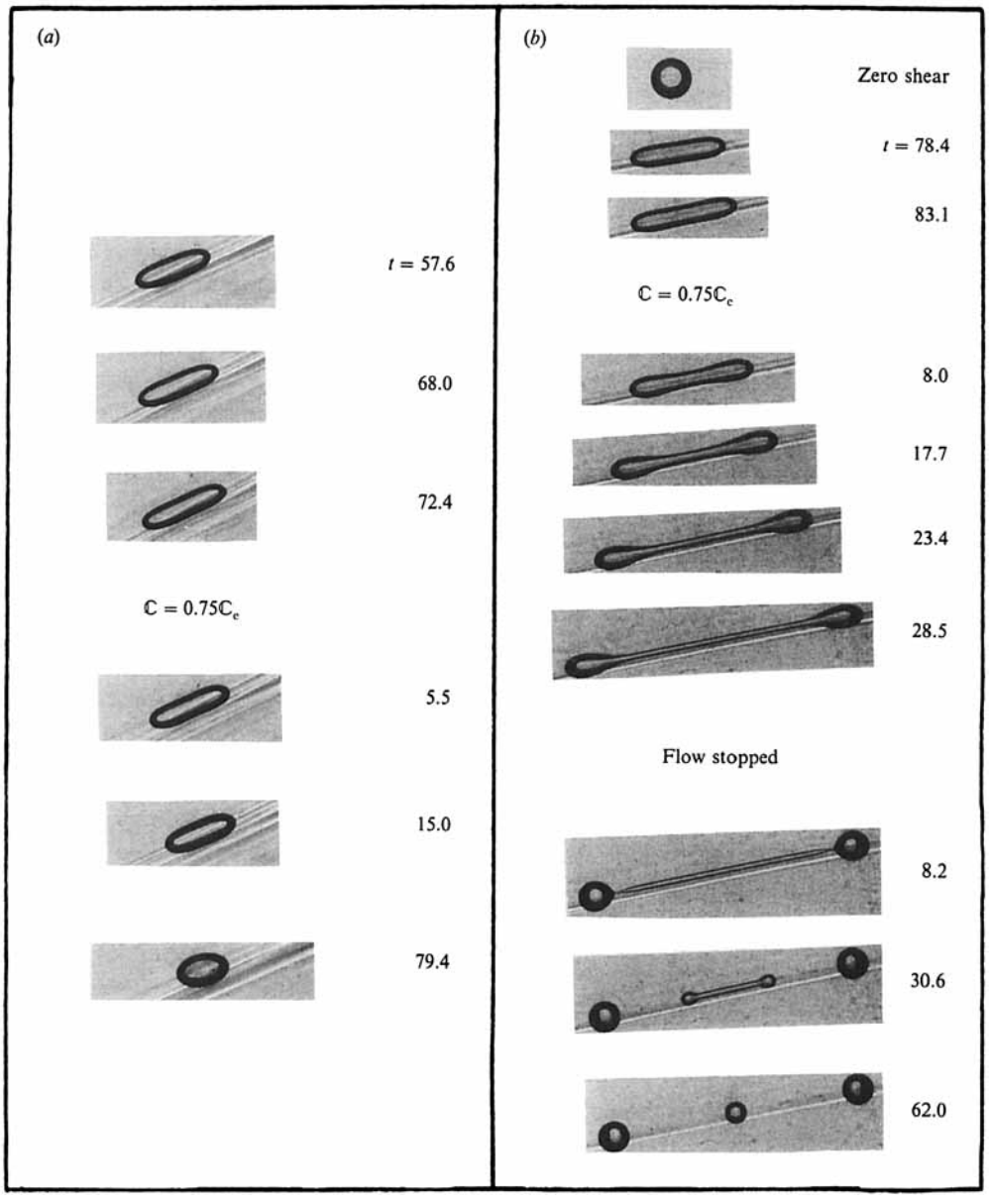

FIGURE 4. The effect of a step reduction in shear rate; the flow type is maintained constant. $\lambda = 1.3$; (*a*) $\alpha = 0.2$; (*b*) $\alpha = 0.6$. Step change from $\mathbb{C}_c$ to $0.75\mathbb{C}_c$.

In the figures, each type of symbol denotes the transient behaviour of a single droplet and the horizontal arrows indicate the elongation at which a step change is made from critical to subcritical flow conditions. The initial transient stretching is very slow and is followed by a rapid elongation when $L/a > 3$. In both figures, one case is shown in which the change to subcritical flow conditions results in the droplets recovering to a steady shape. However, for each viscosity ratio, a larger initial extension leads to breakup. As shown pictorially in previous figures, during the breakup process the end-to-end drop length may either remain the same or noticeably shorten for a significant period of time. This is followed by a period of

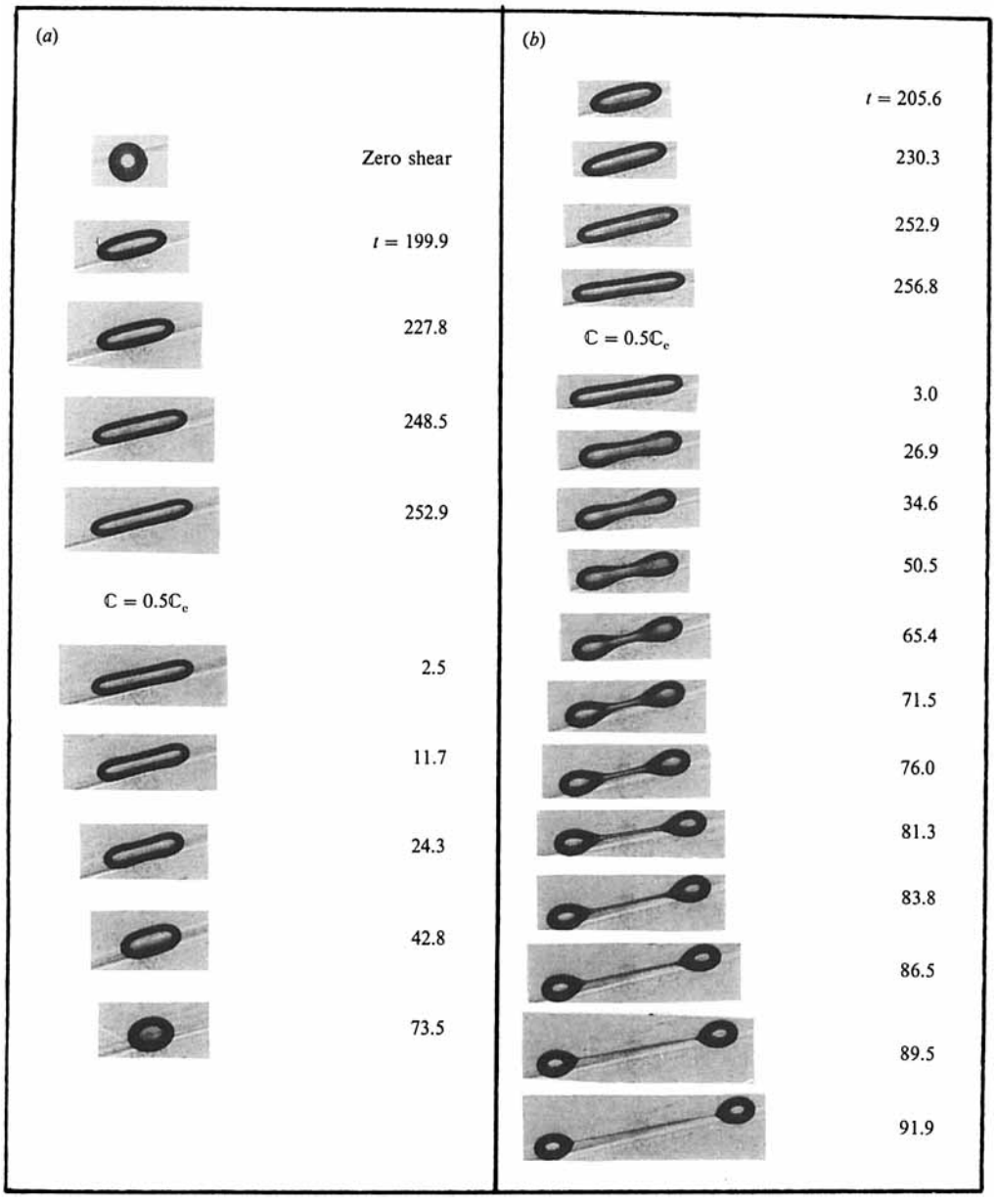

FIGURE 5. The effect of a step reduction in shear rate; the flow type is maintained constant. $\lambda = 5.3$; $\alpha = 0.4$. Step change from $\mathbb{C}_c$ to $0.5\mathbb{C}_c$.

continued stretching, which leads, in the cases shown in figure 6(*a*), to breakup in the flow when the symbols terminate. The high-viscosity-ratio experiments shown in figure 6(*b*) are characterized by stretching with the formation of a thinning cylindrical midsection, but breakup did not occur during the time the drops remained within the linear flow region of the device. The continuous stretching mode is generally observed for the more viscous drops as a necessary precursor to fragmentation, since the internal flow that leads to the pinch phenomenon is damped. We shall discuss this aspect of the breakup of viscous drops more fully using the numerical simulations,

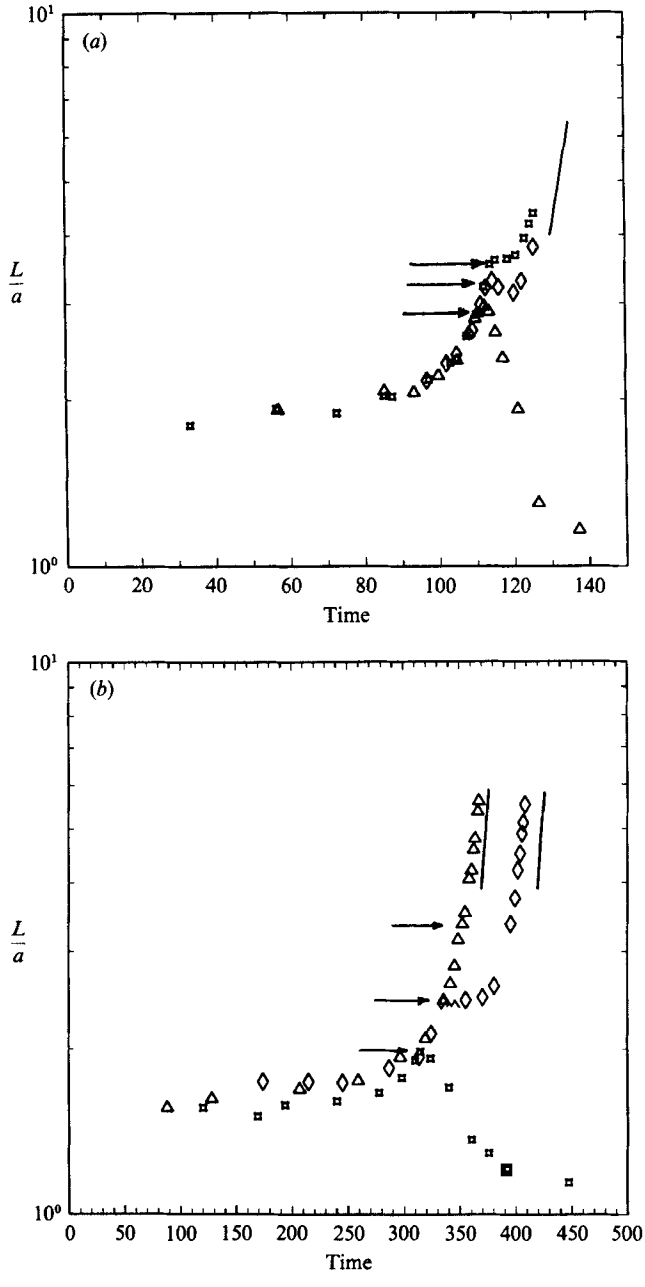

FIGURE 6. Elongation ratio L/a as a function of time for (*a*) $\lambda = 0.1$, $\alpha = 1.0$; (*b*) $\lambda = 5.3$, $\alpha = 1.0$. The horizontal arrows indicate when a step change in shear rate occurs to the new conditions (*a*) $\mathbb{C} = 0.5\mathbb{C}_c$; (*b*) $\mathbb{C} = 0.75\mathbb{C}_c$. The solid line denotes asymptotic stretching similar to a fluid element in the new flow conditions.

§8. The slope of the vertical lines adjacent to the stretching data in figure 6 denote a rate of stretching equal to a line element of the fluid in the new flow conditions. After the period of adjustment to the weaker flow, the droplet again begins to rapidly stretch at a rate that asymptotes to that of a fluid element in the new flow conditions. Finally, in the cases where relaxation back to a steady shape occurs, the drop length

New flow conditions	Critical elongation for breakup
$0\mathcal{C}_c$	$3.4 < \frac{L}{a} < 4.5$
$0.2\mathcal{C}_c$	$3.14 < \frac{L}{a} < 3.35$
$0.4\mathcal{C}_c$	$2.93 < \frac{L}{a} < 3.2$
$0.65\mathcal{C}_c$	$2.44 < \frac{L}{a} < 2.66$
$0.9\mathcal{C}_c$	$2.08 < \frac{L}{a} < 2.25$
Final steady shape	$\frac{L}{a} \approx 1.6$

TABLE 1. The critical elongation necessary for breakup as a function of a change from stretching at the critical capillary number to subcritical flow conditions; step reduction in shear rate only. $\lambda = 0.46$.

decreases monotonically and we have made no observations (experimentally or numerically) of any behaviour similar to the 'inertial overshoot' discussed by Kang & Leal (1987) for the finite-Reynolds-number problem.

4.3. *Varying the magnitude of the step change in shear rate*

The experiments just outlined imply that the capillary number necessary to produce breakup is dependent on the initial drop shape, as indicated by the elongation ratio L/a at the time the flow field is changed, but is otherwise independent of the flow history (assuming, of course, that this history does not lead to drastically different drop shapes that cannot be parameterized by L/a). This behaviour is entirely consistent with the properties of Stokes equations for which the instantaneous velocity field, and consequently the drop shape evolution, depend only on the instantaneous imposed flow and shape. The history of the flow is only important insofar as it produces a definite initial shape. An important question is the dependence of the critical elongation on the magnitude of the step change in the capillary number. Two typical sets of experimental results for the dependence of the critical extension ratio necessary for breakup (either complete fragmentation or breakup via the continuous stretching mode) as a function of the magnitude of the step change in shear rate are summarized in table 1 for the case $\lambda = 0.46$ and in table 2 for the case $\lambda = 5.3$. Qualitatively, the weaker the external flow, the more extended the drop must be to cause breakup. As noted earlier, the results in tables 1 and 2 hold for all flow types ($\alpha > 0$) provided the flow history consists of a step reduction in shear rate only. Perhaps the most significant aspect of the data in these two tables is the fact that even a weak flow can produce breakup for $\lambda = 5.3$, generally via the continous stretching mode, without requiring a large initial elongation, in spite of the fact that an elongation $L/a \approx 8$ is necessary to guarantee breakup if the flow is stopped completely. These results demonstrate that even weak extensional flows can lead to the continuous stretching and breakup of a viscous drop that has a modest initial deformation.

New flow conditions	Critical elongation for breakup
$0\mathbb{C}_c$	$7.6 < \frac{L}{a} < 8.2$
$0.35\mathbb{C}_c$	$3.21 < \frac{L}{a} < 3.38$
$0.5\mathbb{C}_c$	$2.57 < \frac{L}{a} < 2.95$
$0.75\mathbb{C}_c$	$2.0 < \frac{L}{a} < 1.6$
Final steady shape	$\frac{L}{a} \approx 1.6$

TABLE 2. The critical elongation necessary for breakup as a function of change from stretching at the critical capillary number to subcritical flow conditions; step reduction in shear rate only. $\lambda = 5.3$.

4.4 *Effect of viscosity ratio*

Finally, we address the effect of viscosity ratio with particular attention given to larger viscosity ratios. In our previous study (Stone *et al.* 1986), which only investigated transient behaviour following an abrupt halt of the flow, the effect of high viscosity ratios was to severely damp the internal motion which leads to the development of a neck and thus to breakup via the end-pinching mechanism. Consequently, very much larger extensions were necessary to guarantee breakup of viscous drops ($\lambda \gtrsim 5$) in an otherwise quiescent fluid relative to cases with $\lambda = O(1)$. However, as illustrated above in table 2, figure 5 and figure 6(*b*), if the flow is not altogether stopped, but rather reduced to a subcritical value, even modest elongations can lead to drop breakup. Furthermore, the experimental data presented so far suggest that the critical extension necessary to guarantee breakup or, at least, to continue the stretching process, appears to become almost independent of λ for $\lambda > O(1)$. This behaviour is further illustrated in figure 7 where the experimental results for a step change to $\mathbb{C} = 0.75\mathbb{C}_c$, covering three orders of magnitude of viscosity ratio, are summarized. The open symbols refer to complete cessation of flow, and denote the largest elongation ratio for which the drop relaxes back to a sphere (the squares) and the smallest elongation for which breakup was observed (the triangles). Similarly, the filled symbols refer to a decrease in $\mathbb{C}$ to $0.75\mathbb{C}_c$. In this case, the squares represent relaxation back to a steady shape and the triangles represent breakup, either via complete fragmentation in the flow or breakup by the continous stretching mode. The dotted line denotes the maximum elongation of the most deformed steady shapes observed by Bentley & Leal (1986*b*). As tables 1 and 2 document, the qualitative response to a step change in the velocity gradient illustrated in figure 7 is representative of a wide range of step sizes. In spite of the fact that the critical extension for onset of breakup is independent of λ for $\lambda > O(1)$, however, it is nonetheless true that complete fracturing in the flow takes a much longer time for large λ and is most often accompanied by large-scale stretching. In this regard, the actual breakup of viscous drops via flow is still seen to be more

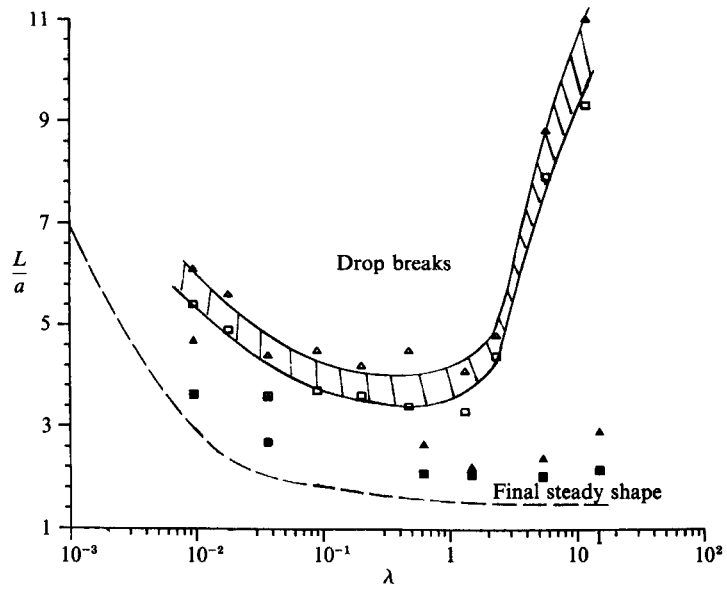

FIGURE 7. Critical elongation ratio necessary to ensure breakup as a function of viscosity ratio. Both an abrupt halt of the flow ($\mathbb{C} = 0\mathbb{C}_c$) and a step change in shear rate to the new flow conditions $\mathbb{C} = 0.75\mathbb{C}_c$ are examined. The open triangles denote the smallest L/a for which a drop was observed to breakup and the open squares denote the largest L/a for which a drop relaxed back to a steady (spherical) shape when the flow was abruptly stopped. The filled triangles and squares represent similar behaviour for the case that the change is made to the subcritical conditions $\mathbb{C} = 0.75\mathbb{C}_c$.

difficult for drops with large λ-values than for drops with $\lambda = O(1)$. It is perhaps worth emphasizing again that all of these conclusions remain true for all flow types with $\alpha > 0$, provided the flow history consists of a simple step change in shear rate.

5. Experimental results: step changes in flow type

We have examined time-dependent dynamics associated with step changes in shear rate. An equally important question is how the drop shape evolution is influenced by changes in flow type. Here we specifically address questions concerned with abrupt changes in flow type, with the shear rate being maintained constant, so that the new flow conditions are subcritical. Recall that as the flow type changes from a hyperbolic flow ($\alpha = 1.0$) towards a simple shear flow ($\alpha = 0$), the addition of vorticity causes a drop to rotate away from the principal axis of strain. Thus, the effective shear rate experienced by the drop is reduced and the effective capillary number becomes subcritical. Again, in these experiments changes in flow conditions are applied with a drop undergoing a transient stretching at the critical capillary number. The computer-controlled four-roll mill in our laboratory is one of the few (only?) devices currently capable of performing such a study in a well-controlled manner.

Figures 8, 9 and 10 show the effects of a step change in flow type for three different viscosity ratios, $\lambda = 0.1$, 1.3 and 5.3, respectively. These photographs are typical of the experimental results. The breakup processes are obviously similar to those

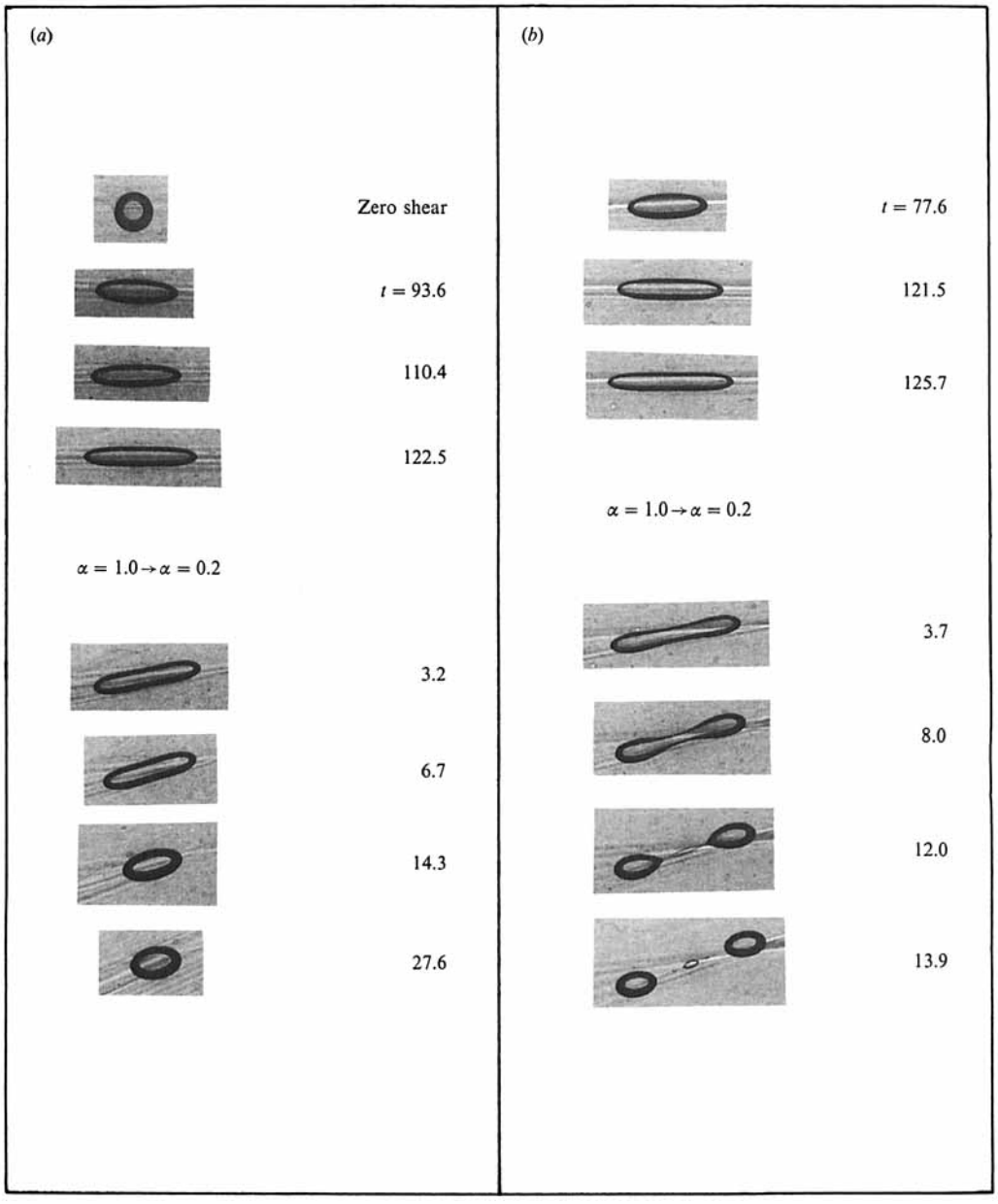

FIGURE 8. The effect of a step change in flow type; the shear rate is maintained constant. $\lambda = 0.1$. Step change from $\alpha = 1.0$ to $\alpha = 0.2$.

described in figures 1–7. In figures 8–10 the step change in flow type is followed by rapid rotation to a steady orientation after which the observed behaviour is either (1) relaxation back to a steady shape, (2) breakup in the flow without large-scale stretching or (3) continued stretching and breakup. No new steady shapes are observed and the steady orientation achieved by the droplets is along the outflow axis of the new flow field. The rotation process is documented clearly in figure 10.

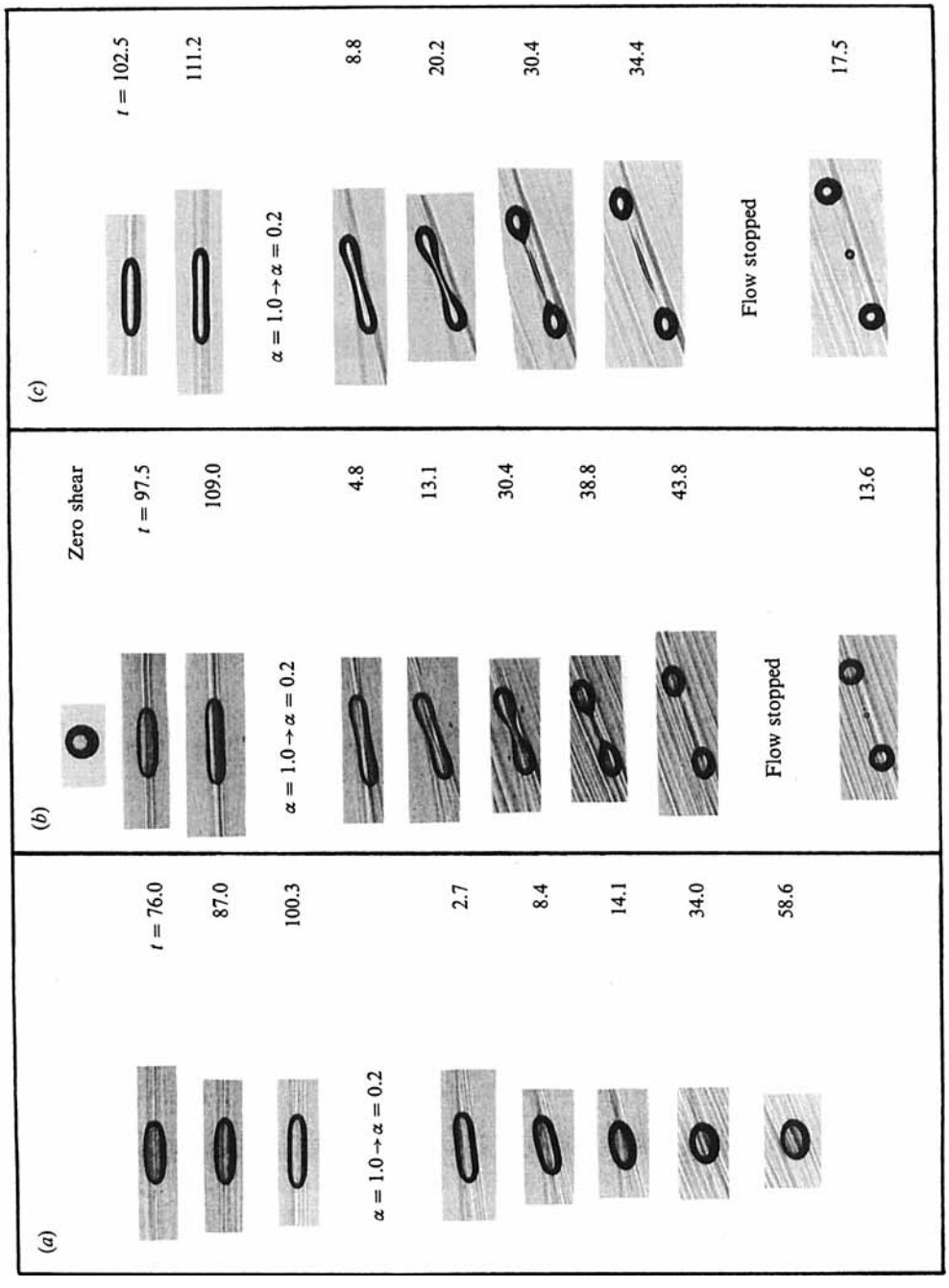

FIGURE 9. The effect of a step change in flow type; the shear rate is maintained constant. $\lambda = 1.3$. Step change from $\alpha = 1.0$ to $\alpha = 0.2$.

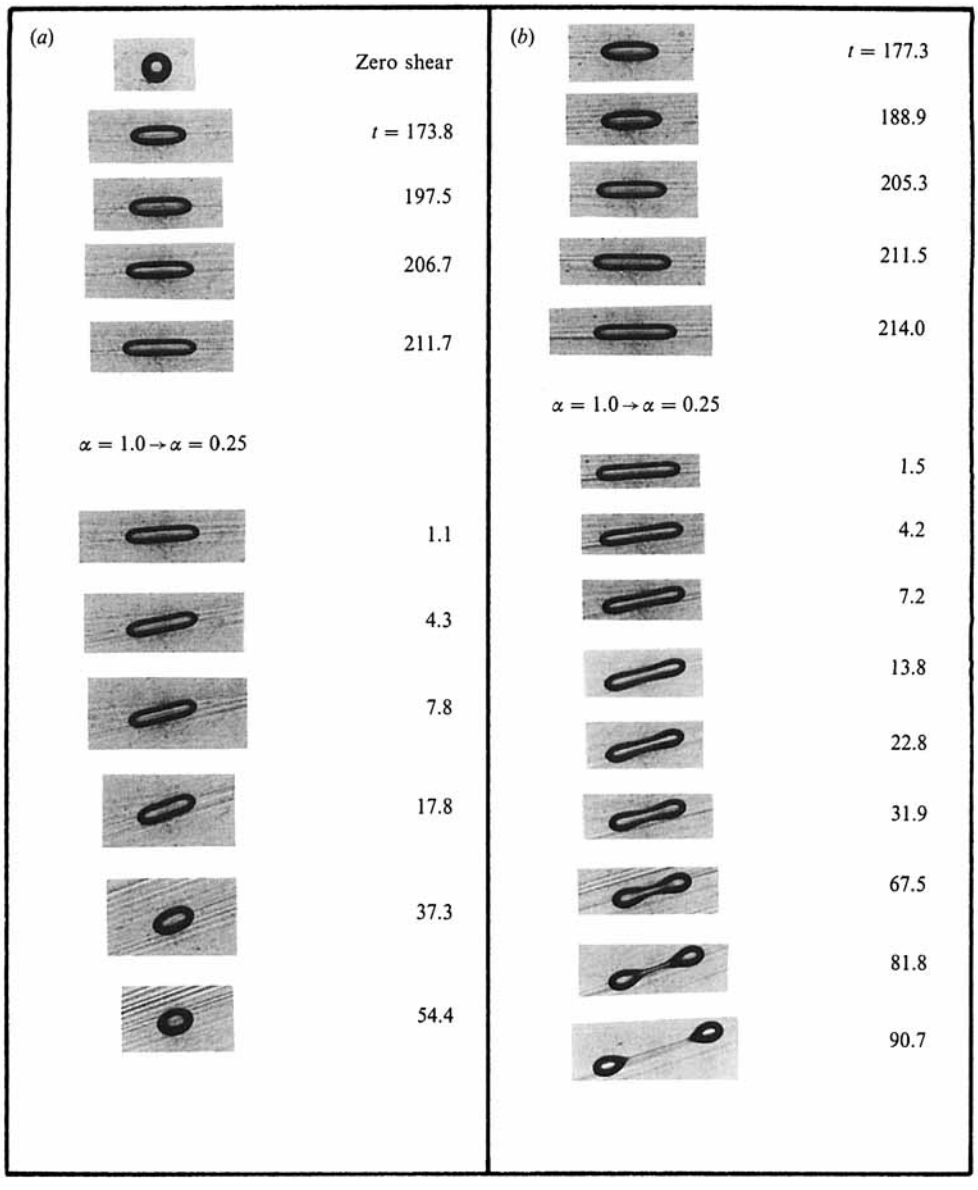

FIGURE 10. The effect of a step change in flow type; the shear rate is maintained constant. $\lambda = 5.3$. Step change from $\alpha = 1.0$ to $\alpha = 0.25$.

Clearly, the most significant new dynamical feature associated with the sudden addition of vorticity is that for these modest deformations and the small capillary numbers at which the step change occurs, drop rotation appears very rapid relative to any significant deformation.†

† As an aside, for those readers interested in geometric aspects of free surfaces, the photograph of the droplet just as it is fracturing in figure 8(*b*) shows a narrow conically shaped central thread attached to an almost spherical droplet. This is very similar to an observation of Peregrine

As a consequence of this rapid rotation, relative to any significant interfacial-tension-induced change of shape, the drop aligns along the outflow axis where the effective shear rate is $G\alpha^{\frac{1}{2}}$. Thus, the introduction of a step change in vorticity appears to be equivalent to a step change in shear rate from $\mathbb{C}_c$ to a reduced value equal to $\alpha^{\frac{1}{2}}\mathbb{C}_c$. An obvious question is then whether the critical extension L/a, necessary for breakup, remains the same for the same fractional decrease in capillary (or effective capillary) number.

We have not performed a large number of experiments to explore this point. However, in all the experiments performed, the critical length for breakup, given only a step change in shear rate G, is nearly the same as for a given change in $\alpha^{\frac{1}{2}}$. For example, in experiments with $\lambda = 0.46$, a step change from $\alpha = 1.0$ to $\alpha = 0.4$ ($\alpha^{\frac{1}{2}} = 0.63$) showed rapid rotation to the new steady orientation along the outflow axis and a critical extension ratio for breakup $2.35 < L/a < 2.57$, which compares very well with the data illustrated in table 1 for a change in G to $0.65G_c$. This suggests that for these modestly extended drops, step changes in either G or α will have a comparable effect provided that they correspond to the same change in $G\alpha^{\frac{1}{2}}$. The dynamical reason for this suggestion is the fact that the droplet is oriented along the outflow axis (the eigenvector) of the new flow during almost the entire period of the transient change in shape. If correct, it implies that when both shear rate changes and flow type changes occur simultaneously, the critical extension ratio for breakup should depend only on the effective capillary number in the modified flow $\mathbb{C}_{\text{eff}} = G\alpha^{\frac{1}{2}}\mu a/\sigma$.

The observation that a sudden addition of vorticity leads to rapid rotation relative to any significant drop deformation, at least for $\lambda = O(1)$, may appear somewhat surprising. Although a general analytic solution is not available for the orientation of a finitely deformed drop in a linear flow, useful ideas can be obtained by considering a solid ellipsoid of revolution (cf. Bentley & Leal 1986*b*). A solid particle in a linear shear flow will have an angular velocity proportional to G, so the time to rotate from an initial orientation to a final steady orientation should scale with the inverse of the shear rate G^{-1}. This is comparable with the timescale for deformation only if the droplet is highly extended, in which case the drop is observed to extend at a rate similar to a fluid element in the flow. The key fact with regard to our observations in these experiments is that the stretching process at the critical capillary number is very slow initially (see the discussion in Stone *et al.* 1986) and the droplet does not begin to behave similarly to a fluid element until $L/a > 3$. Typically, for a rapid addition of vorticity when the droplet is only modestly deformed (say, $L/a \approx 2$–3, as in these experiments), the timescale for deformation is much longer than G^{-1} (see figure 6) and the rotation to a new orientation can be decoupled from the deformation process. Once the drop is reoriented, however, the effective shear rate in the new flow is $G\alpha^{\frac{1}{2}}$ (Bentley & Leal 1986*b*).

(1986) on the shape of the liquid bridge joining a nascent drop to the remainder of the fluid, although viscous effects in Peregrine's experiments are generally insignificant. The conical interface is also very similar to intermediate shapes observed in the formation of satellite drops due to capillary wave growth on cylindrical fluid interfaces (Goedde & Yuen 1970 and Van Dyke 1982). It suggests that conically shaped surfaces created during the evolution of fracturing interfaces may be a general geometrical phenomena. Additional examples can be seen in figures 2–5 and figure 11(*b*, *c*). However, we have not investigated this matter further.

6. Experimental results: simultaneous step changes in shear rate and flow type

In order to further test the idea of an effective capillary number

$$\mathbb{C}_{\text{eff}} = G\alpha\mu a/\sigma = \mathbb{C}\alpha^{\frac{1}{2}}$$

for describing the dynamics of drops in the simple transient flows studied here, we present some experimental observations on simultaneous step changes in shear rate and flow type. First, it should be re-emphasized that the validity of the correlation of drop behaviour and an effective capillary number depends on the disparate timescales governing different aspects of the dynamics. Because the drop shape evolution depends on the global shape rather than details of the shape, then, provided rotation to a new steady orientation is sufficiently fast relative to the timescale for any significant overall deformation (due either to interfacial tension or an external flow), the breakup criteria can be stated entirely in terms of the initial elongation L/a and an effective capillary number $\mathbb{C}_{\text{eff}}$.

In figure 11 (a, b) we show the results of step changes from an initial condition $\mathbb{C} = \mathbb{C}_c$ and $\alpha = 1.0$ to a final condition $\mathbb{C} = 0.8\mathbb{C}_c$ and $\alpha = 0.6$. Figure 11 (c) illustrates the effect of a step increase in the actual capillary number to $\mathbb{C} = 1.3\mathbb{C}_c$ but with the flow type changed from $\alpha = 1.0$ to $\alpha = 0.25$ so that the effective capillary number is reduced. The drops in figure 11 have a viscosity ratio $\lambda = 0.46$. In the first case (figure 11a, b) the effective capillary number characterizing the new flow conditions is $\mathbb{C}_{\text{eff}} = 0.62\mathbb{C}_c$ and in the latter case (figure 11c) $\mathbb{C}_{\text{eff}} = 0.65\mathbb{C}_c$. As discussed in the description of the experiment (§3), the time for flow field modification following a step change in flow conditions is fast compared with the time typical of the drop deformation and rotation and this is also true for the 30% step increase in shear rate studied here.

We make the following observations concerning the effects of simultaneous changes in shear rate and flow type. In figure 11 (a), after the step change in flow conditions, the droplet relaxes back to a steady shape. However, during the relaxation process, the droplet develops a 'waist' due to the external flow trying to drain fluid from the drop centre. Eventually, though, the relaxational motion, driven by the ends, dominates and a steady shape is established. Figure 11 (b) illustrates the effect of a slightly more elongated initial shape. The droplet first reorients prior to any significant deformation, then breaks in the subcritical steady flow in a manner reminiscent of many of the earlier figures.

In figure 11 (c), as the droplet rotates away from the extensional axis, it initially feels a stronger effective shear rate since the shear rate was increased to $1.3G_c$. The droplet reorients and deforms a little, then rapidly begins to stretch and eventually fractures in the flow.† Again, we observe a conically tipped thread at the end of the central portion of the droplet connected to the deformed spherical end shortly before the final fragmentation is complete. After the flow is stopped the central thread relaxes and fragments leaving the small satellite drops shown in the last photograph. Figure 11 (b, c) appears to be very close to the critical length for breakup which we estimate in both cases to be $L/a \approx 2.4$–2.6. This estimate of the critical length for breakup at $\mathbb{C}_{\text{eff}} = 0.65\mathbb{C}_c$ is in good agreement with the data reported in table 1 that accounts only for a step change in shear rate.

† The size of the drop shown in figure 11 (c) is smaller than the drop in figure 11 (a), but the dimensionless elongation ratio L/a at the time the flow field is changed is slightly larger.

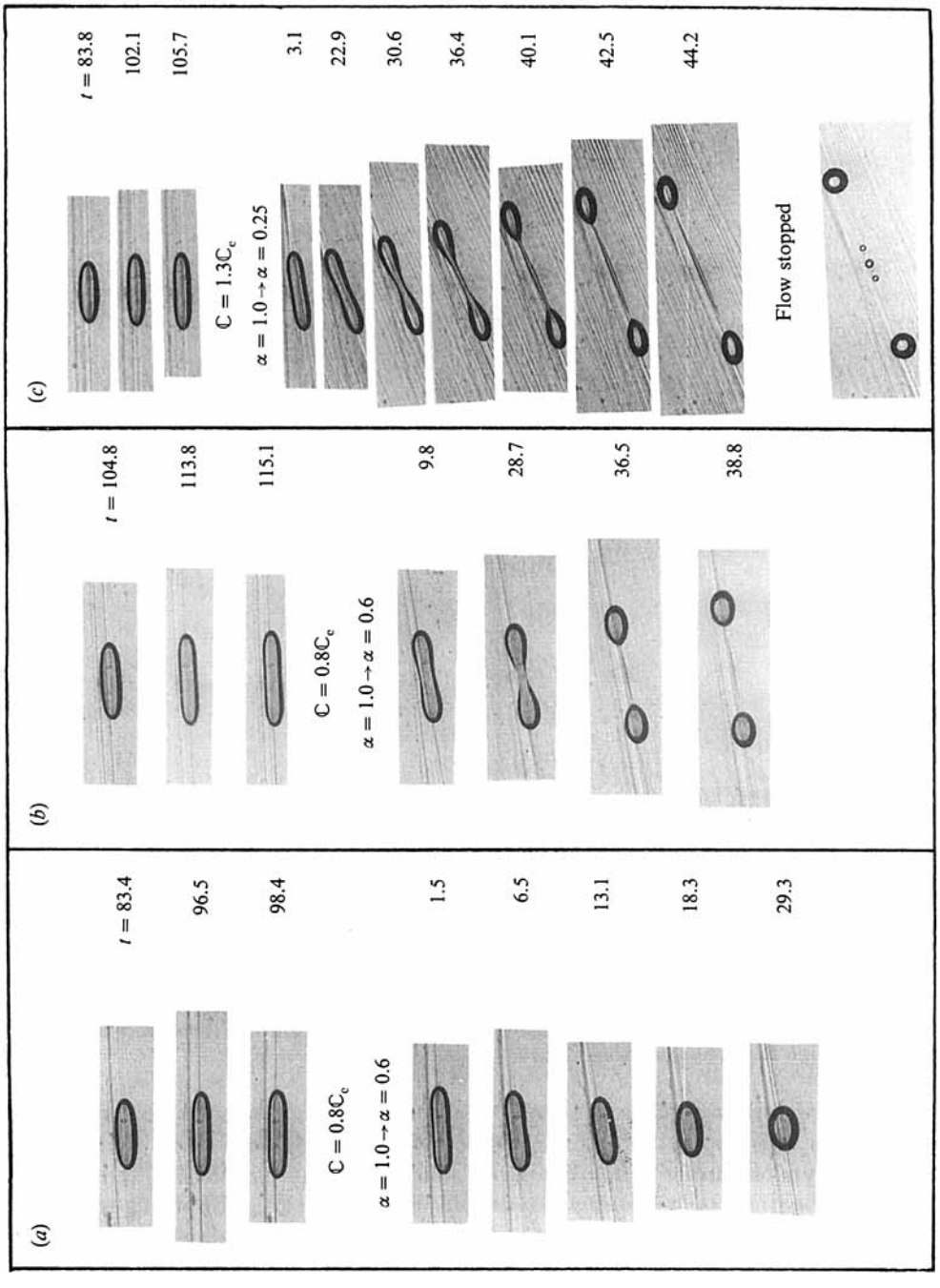

FIGURE 11. The effect of a simultaneous change in shear rate and flow type. $\lambda = 0.46$. (*a*, *b*) Step changes from $\mathbb{C}_c$ to $0.8\mathbb{C}_c$ and $\alpha = 1.0$ to $\alpha = 0.6$. (*c*) Step changes from $\mathbb{C}_c$ to $1.3\mathbb{C}_c$ and $\alpha = 1.0$ to $\alpha = 0.25$.

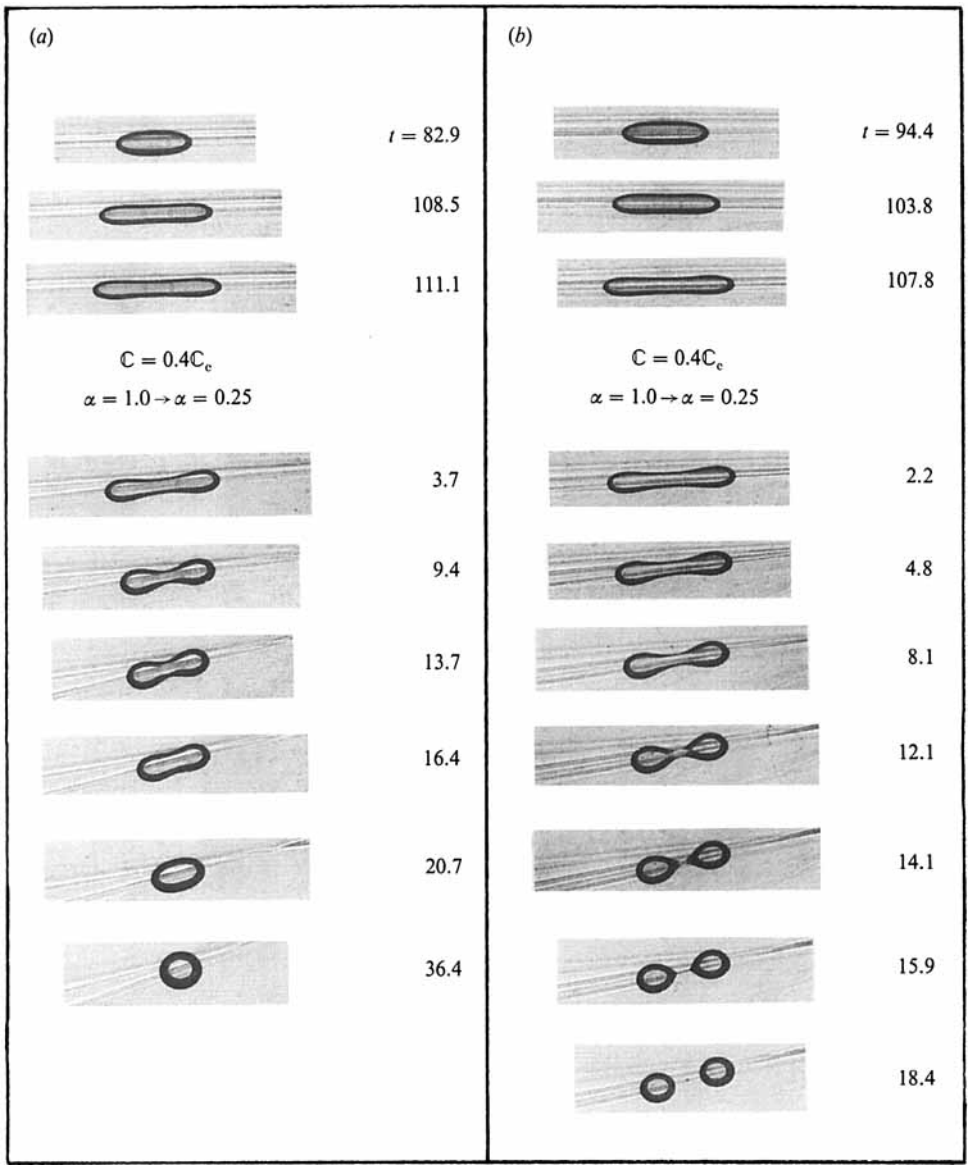

FIGURE 12. The effect of a simultaneous change in shear rate and flow type. $\lambda = 0.46$. Step changes from $\mathbb{C}_c$ to $0.4\mathbb{C}_c$ and $\alpha = 1.0$ to $\alpha = 0.25$.

In figure 12 we show another sequence of simultaneous changes in flow type and shear rate. For this droplet, $\lambda = 0.46$, the shear rate is reduced from G_c to $0.4G_c$ and the flow type simultaneously changed from $\alpha = 1.0$ to $\alpha = 0.25$. The effective capillary number at the new flow conditions is $\mathbb{C}_{\text{eff}} = 0.2\mathbb{C}_c$. First, figure 12(*a*) provides an example of a waist forming initially due to the external extensional flow, only to eventually be overwhelmed by the inward capillary-driven flow generated by the bulbing ends. Figure 12(*b*) appears to be very close to the critical length necessary for breakup as the droplet fractures in two with a very small satellite droplet in between. Also, the droplet has a shorter end-to-end length at breakup than the initial length at the time the step change in flow conditions occurs. The critical length for

breakup, as bounded by the two sets of photographs in figure 12, is $3.2 < L/a < 3.3$, which is again in good agreement with the data in table 1. Therefore, it appears clear from the experiments performed using simultaneous step changes in flow conditions, in conjunction with the effect of viscosity ratio, shear rate and flow type described in §§ 4 and 5 that the effective capillary number at the new flow conditions is useful for predicting breakup behaviour for a given initial shape, provided only that droplet rotation to a steady orientation is sufficiently fast.

One should expect that the above timescale assumptions would begin to break down for a sufficiently large increase in G and a corresponding decrease in $\alpha^{\frac{1}{2}}$, based upon the supposition that the drop would spend a significant length of time in a very strong flow as it rotates to the final steady orientation. Nevertheless, at least in the case illustrated in figure 11 (*c*), the breakup behaviour was still well correlated with $\mathbb{C}_{\text{eff}}$. The viscosity ratio will also play a role in such timescale arguments as viscous drops deform more slowly than lower-viscosity-ratio drops. In the case of large viscosity ratios, the difference between reorientation and deformation timescales will be even larger than illustrated in figures 11 and 12, and the idea of an effective capillary number should be even better for very viscous droplets. However, inviscid drops ($\lambda \ll 1$) are characterized by very long, slender shapes with nearly pointed ends and, in response to a subcritical flow, the relaxational motion, driven by large curvature variations near the ends, occurs on a timescale comparable with the rotation time so that the idea of disparate timescales breaks down in this case. From the above arguments we conclude that the critical extension data tabulated in tables 1 and 2 and figure 7, which were determined from experiments involving step changes in shear rate only, should be equally useful for the broader class of flows involving simultaneous changes in shear rate and flow type, provided only that the interpretation is based upon the effective critical capillary number $\mathbb{C}_{\text{eff}}$ as described above, and the drops are not initially too deformed (i.e. $L/a < 3$).

7. Experimental results: breakup for large λ in weak flows with vorticity

As pointed out by Taylor (1934) for the case of simple shear flow, the effect of vorticity in a steady flow is to inhibit breakup of a drop which is initially spherical or nearly spherical in shape. Indeed, for sufficiently high viscosity ratios, droplets attain a maximum steady deformation in all two-dimensional flows with vorticity and any additional increases in capillary number are only accompanied by increased rotation of droplet fluid rather than by any noticeable deformation. For example, in simple shear flow, breakup is not possible if the viscosity ratio exceeds approximately 4 and for $\alpha = 0.2$ and 0.4 breakup is not possible for viscosity ratios above approximately 20 and 60, respectively (Bentley & Leal 1986*b*).

An obvious question in the context of the present study is whether high-viscosity-ratio drops can be broken in flows with vorticity if the initial deformation exceeds the maximum stable deformation that is observed in the steady-state experiments. Clearly, if viscous drops are very highly extended prior to application of a flow with vorticity, previous photographs and discussion in this paper should suggest that breakup would be possible if the product $G\alpha^{\frac{1}{2}}$ is sufficiently large. Here, we consider an initial condition that is more deformed than the maximum steady deformation, but still not highly stretched.

In figure 13 we report the results of an experiment for $\lambda = 19$. For reference, at the top of the figure we show a photograph of the maximum steady deformation attainable by beginning with a spherical drop and increasing the capillary number in

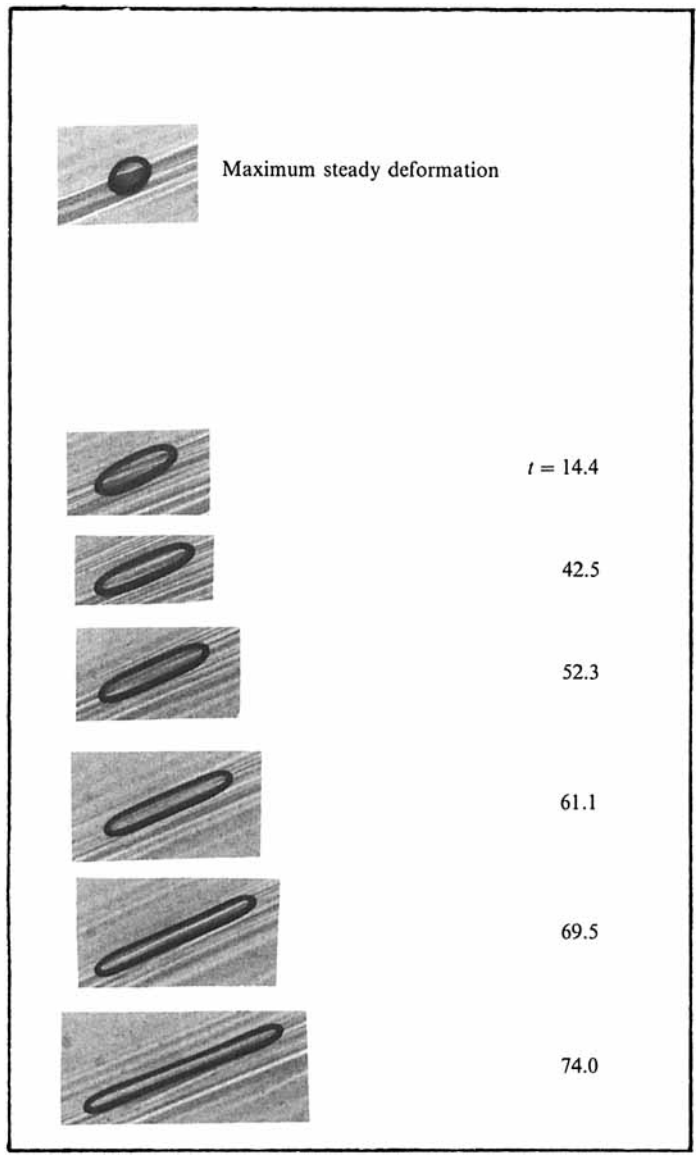

FIGURE 13. Breakup of a very viscous droplet beginning with a shape that exceeds the maximum steady deformation. $\lambda = 19.0$, $\alpha = 0.2$, $\mathbb{C} = 0.3$. If the initial shape were spherical, no breakup would occur and the droplet would reach a limiting deformation shown by the first photograph. In such instances, increases in capillary number only lead to more rapid fluid rotation rather than increasing deformation.

small increments (i.e. the steady experiment described by Bentley & Leal 1986*b*). In the bottom part of the figure, we examine the breakup of the same drop in the same flow when the drop is first deformed to a more highly elongated initial shape by a stronger flow. The initial elongated shape is generated by stretching the drop in a purely extensional flow ($\alpha = 1.0$) at the critical shear rate so that unsteady stretching occurs. Then, the flow is abruptly stopped, the droplet begins to relax and a steady flow field with $\alpha = 0.2$ is applied. The photographs shown illustrate that the droplet

reorients along the outflow axis of the $\alpha = 0.2$ flow and continues to stretch. It must be remarked that the rate of elongation, produced by this weak flow coupled with the high viscosity ratio, is very slow. The experiment does not represent the lowest possible capillary number for breakup given the non-spherical initial condition, but does show that different initial conditions, even modest initial deformation, can lead to breakup of very viscous drops where simple steady approaches to breakup would never succeed.

8. Numerical study of step changes

The numerical study we present here is designed to complement the basically qualitative description of the dynamics that was demonstrated by the series of experiments described in the preceding sections. The numerical simulations illustrate systematically the detailed features of the external and internal flow fields during the evolution of the drop shape. Also, in these step-reduction studies, it is straightforward to vary the magnitude of the subcritical flow for precisely the same initial shape or to vary the initial shape for an instantaneous change to a given subcritical flow, and both types of simulations are shown below.

8.1. *Numerical procedure*

A powerful numerical scheme for this type of free-boundary problem is the boundary-integral method, first applied to the drop deformation problem by Rallison & Acrivos (1978). This method is particularly suitable as only the drop surface needs to be discretized rather than the entire domain and, consequently, interfacial velocities are calculated directly. Details of the application of the method to the drop deformation problem can be found in Stone & Leal (1989). The interfacial velocity is calculated from the integral equation

$$\tfrac{1}{2}(1+\lambda)\,\hat{\boldsymbol{u}}(\boldsymbol{x}_s)+\frac{3}{4\pi}(1-\lambda)\int_{S(t)}\boldsymbol{n}\cdot\left[\frac{(\boldsymbol{x}_s-\boldsymbol{y})(\boldsymbol{x}_s-\boldsymbol{y})(\boldsymbol{x}_s-\boldsymbol{y})}{|\boldsymbol{x}_s-\boldsymbol{y}|^5}\right]\cdot\hat{\boldsymbol{u}}(\boldsymbol{y})\,\mathrm{d}S$$
$$=\mathbb{C}\boldsymbol{\Gamma}\cdot\boldsymbol{x}_s+\frac{1}{8\pi}\int_{S(t)}(\nabla_s\cdot\boldsymbol{n})\,\boldsymbol{n}\cdot\left[\frac{I}{|\boldsymbol{x}_s-\boldsymbol{y}|}+\frac{(\boldsymbol{x}_s-\boldsymbol{y})(\boldsymbol{x}_s-\boldsymbol{y})}{|\boldsymbol{x}_s-\boldsymbol{y}|^3}\right]\mathrm{d}S, \quad (4)$$

where $\nabla_s\cdot\boldsymbol{n}$ represents the mean curvature of the surface S, $\boldsymbol{n}$ is the unit normal directed from the droplet phase to the suspending phase and $\boldsymbol{x}_s$ denotes a point on the fluid–fluid interface, $\boldsymbol{x}_s\in S$. In this equation, all velocities have been non-dimensionalized with respect to $u_c = \sigma/\mu$, lengths with respect to the undeformed radius $l_c = a$ and time by the convective timescale $t_c = l_c/u_c$. Also, $\boldsymbol{\Gamma}$ represents the dimensionless velocity gradient tensor, equation (1), non-dimensionalized with respect to the shear rate $\bar{G}$ prior to the step change.

For the axisymmetric drop shapes we shall examine here, the azimuthal integration is performed analytically so that the surface is reduced to a line integral. Given the drop shape, (4) is an integral equation of the second kind for the unknown $\hat{\boldsymbol{u}}$. This equation is solved by discretizing the surface and converting (4) to an equivalent linear system of equations that is solved by standard Gaussian elimination techniques. The interfacial velocity field is used to evaluate the interior and exterior velocity fields which are helpful in understanding detailed features of the drop shape evolution.

Since the boundary-integral method is derived from the quasi-steady form of Stokes equation, the application of this numerical technique to time-dependent

problems implicitly assumes that inertial effects due to the unsteady nature of the motion are negligible. This is indeed true provided that the timescale for vorticity diffusion, $\rho a^2/\mu$, is much shorter than both the time characteristic of drop deformation, $\mu(1+\lambda)a/\sigma$ and the time representative of convective effects in the external flow, $\bar{G}^{-1}$. Therefore, we require $\rho\sigma a/\mu^2(1+\lambda) \ll 1$ and $\rho\bar{G}a^2/\mu \ll 1$.

8.2. *Changes in initial elongation for given step reduction in G*

We begin by examining droplet extension in a uniaxial extensional flow. Starting with a spherical droplet, the capillary number is increased in small increments until a steady shape no longer exists and a continuous stretching process occurs. Then, at different stages of the elongation process, the capillary number is decreased abruptly to a subcritical value, analogous to the experimental study described in § 4. Two different viscosity ratios are examined, $\lambda = 1.0$ and $\lambda = 10$. The calculations with $\lambda = 1.0$ are especially straightforward and capture all of the important qualitative features of the shape evolution and the velocity field. The study of $\lambda = 10$ is useful for understanding the observed differences in the relaxation and breakup processes for very viscous drops in subcritical flows relative to experiments where the flow is stopped abruptly (Stone *et al.* 1986). Studies of drop deformation in biaxial extensional flows are also straightforward numerically, though not realizable experimentally in the four-roll mill, but these involve a number of new issues that will be discussed in a separate publication (cf. Stone 1988).

In figures 14 and 15, we illustrate the results of our numerical calculations for $\lambda = 1$ and 10, respectively. The solid curves show the time-dependent elongation that occurs at slightly supercritical capillary numbers. The evolution of the drop shape is also shown at intermediate times during the transient stretching process. The shapes are identified by the letters a, b, c, etc. Characteristically, the elongation is very slow initially. But, as a waist develops, the drop begins to stretch rapidly approaching the asymptotic limit of stretching at the rate of a line element of the fluid in the undisturbed flow (the solid nearly vertical line in these figures).

The effect of abruptly decreasing the capillary number at different times during the continuous extension can be seen in figures 14 and 15. In each case, we consider a step change to $\mathbb{C} = 0.5\mathbb{C}_c$ for three different initial conditions. The resulting evolution is shown by the dashed lines in figures 14 and 15 and by the numerically generated shapes that are presented. As indicated in the experimental study, there appear to be three modes of behaviour. In each figure, curve A shows the relaxation back to a steady shape. This is the same steady shape as calculated by beginning with a spherical drop in this subcritical flow. Curve B illustrates the time-dependent breakup mode in which the drop initially shortens in length as the ends become rather bulbous. In figure 14, $\lambda = 1.0$, the formation of a significant neck leads to complete breakup in the flow although the drop has extended very little. In addition, the thin cylindrical thread connecting the two almost spherical ends forms a small satellite drop. This illustrates breakup in a steady flow without large-scale stretching of the drop, similar to several of the experiments discussed in § 4. On the other hand, for $\lambda = 10$, curve B initially shows similar behaviour to $\lambda = 1$, but the tendency toward pinch-off of the ends is inhibited and the drop begins to elongate at the rate of a line element of the fluid. This behaviour corroborates the experimental observation that drops of large viscosity ratio generally do not appear to undergo breakup without first undergoing a large degree of stretch. Finally, for the initial condition used for the curves C, the droplet has a very small initial relaxation as the shape at the end responds to the weaker velocity gradient by becoming more

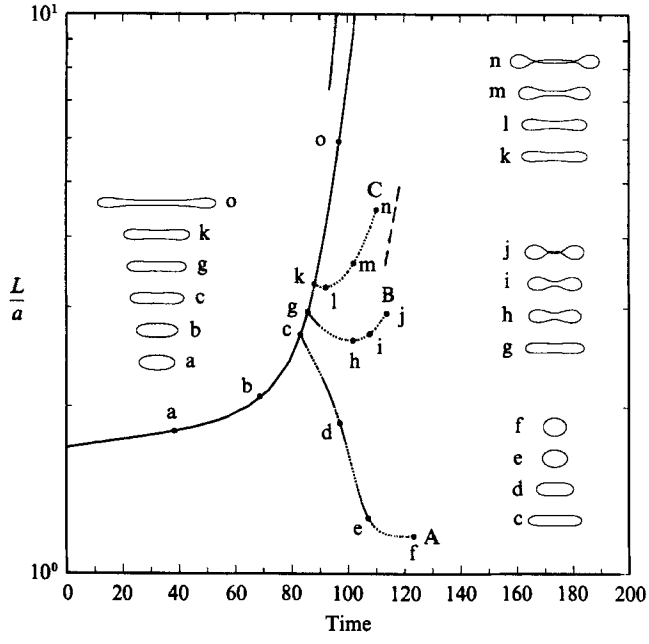

FIGURE 14. Numerical simulation of step changes in capillary number for three different initial conditions. $\lambda = 1.0$; $\mathbb{C}_c$ to $0.5\mathbb{C}_c$. The solid, almost vertical line is the asymptotic limit of stretching like a fluid element in the undisturbed flow. The solid curve is the time-dependent elongation of the droplet at the critical capillary number. The dashed curves are the response to a step change in shear rate to $\mathbb{C} = 0.5\mathbb{C}_c$. The dashed line is the asymptotic limit of stretching like a fluid element in the new flow conditions.

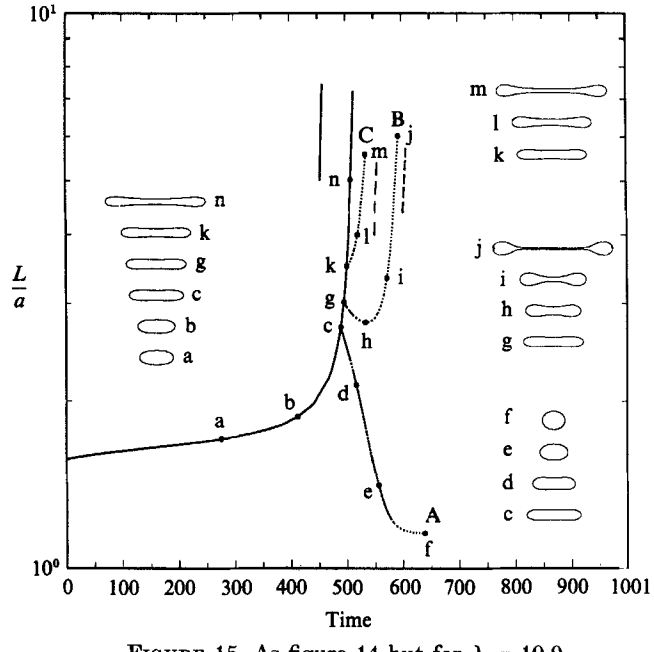

FIGURE 15. As figure 14 but for $\lambda = 10.0$.

bulbous, but without significant shortening prior to undergoing rapid extension. In the case of $\lambda = 1.0$, it is evident that the ends are pinching off, but the drop is simultaneously beginning to stretch. However, the $\lambda = 10$ droplet stretches during the time shown and there is no evidence of the ends breaking off. This is again related to the fact that the flow process internal to the droplet that leads to the end-pinching phenomenon is damped by the more viscous droplet fluid. Consequently, the end-pinching mechanism requires longer times for breakup of high-viscosity-ratio systems so that, instead of fragmentation, deformation in the weak flow is characterized by a significant increase in the end-to-end drop length. Finally, the dashed almost vertical line adjacent to curve C in figures 14 and 15 illustrates the rate at which a fluid element stretches in the new flow conditions. Evidently, the droplet elongation approaches this asymptotic behaviour once it develops a significant waist.

In all cases, the numerical results indicate that the curvature near the end decreases (i.e. the end becomes more rounded) in response to the abruptly weaker flow. This is true even in instances where the drop responds by continuing to stretch, so that the end becomes more spherical as the drop elongates. The simulations also indicate, in agreement with the experimental results discussed in §§ 4–6, that there is a narrow range of initial elongations for which the drop shortens initially, but then eventually stretches again, leading to breakup. Although there are cases in which breakup occurs without stretching owing to the interaction of the extensional flow and the interfacial-tension-driven flow, the range of initial conditions that lead to complete breakup without stretching is extremely narrow for viscous drops in which the flow process leading to end-pinching is inhibited. Nevertheless, in the experimental study, several cases of complete breakup of high-viscosity-ratio drops with relatively little extension have been documented (figures 2, 5 and 10).

8.3. *Evolution of the velocity field during relaxation and breakup*

In order to better understand the evolution of the drop shape, we present the internal and external velocity fields in figures 16 and 17 for the intermediate shapes shown along curve B in figures 14 and 15. The arrows denote the direction and relative magnitude of the fluid velocity, but there is no connection between arrows in one illustration and those in another. The 'competition' between the externally imposed flow and the interfacial-tension-driven flow is clearly evident. For example, the competition between these two mechanisms produces a closed vortical motion interior to the droplet (figure 16*a–c*). Figure 16(*a*) shows the velocity field just after the abrupt change in shear rate. Initially, the most noticeable motion takes place near the ends of the droplet. The ends become more spherical and drive a large inward velocity. Near the droplet centre, the external flow produces an extensional motion which causes the droplet to form a waist and continually thin. The precise role of the interfacial-tension-driven flow field will be examined in detail below. As the end becomes more rounded the driving force for inward motion becomes weaker while the drop continues to thin. In figure 16(*c*) the drop is beginning to lengthen slowly and a visible neck is formed near the bulbous end. This neck will eventually lead to the ends pinching off and the remaining liquid thread in the middle will form at least one satellite drop. At $t = 113.8$ the fluid velocity in the neighbourhood of the pinch is much larger than the speed at which the end translates. This is responsible for pinch off without large-scale stretching of the droplet. At least in the central section of the drop the velocity profile is parabolic, as expected from a slender-body analysis (Acrivos & Lo 1978). Qualitatively, very viscous drops have much flatter interior

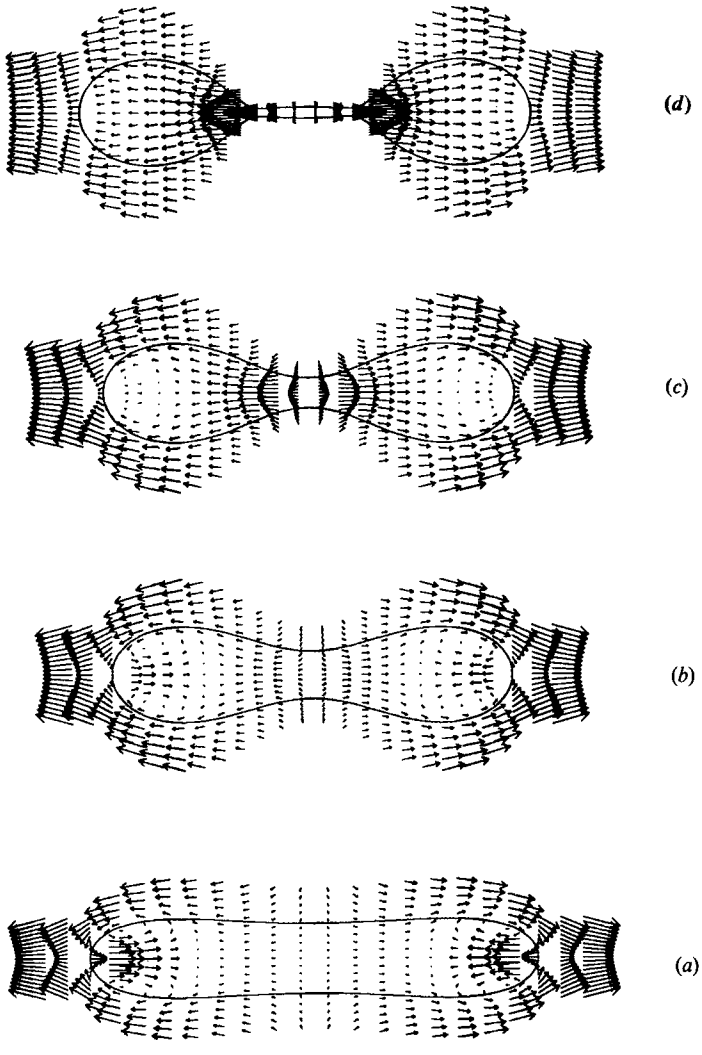

FIGURE 16. Numerical simulation of the internal and external velocity fields during the relaxation and breakup of a droplet after a step reduction in capillary number; $\lambda = 1.0$; $\mathbb{C} = 0.5\mathbb{C}_c$. The simulations correspond to the intermediate shapes shown along curve B in figure 14.

velocity profiles than do smaller viscosity droplets. In the $\lambda = 10$ simulation shown in figure 17 there is no pinch evident. Presumably, for the initial condition chosen, longer times, hence more elongated droplets, are necessary before a significant pinch can develop for this case.

In these stimulations of a step reduction in shear rate, the mechanism of the breakup process can be seen to involve an interaction between an interfacial-tension-drive flow and a flow produced by the external velocity field. The net effect is both competitive and cooperative depending on the region of the drop and the stage of the interface evolution. In order to illustrate this last point we examine the contributions to the two components of the interfacial velocity field (u_r, u_z) at different times during the breakup process for the cases $\lambda = 1.0$ and $\lambda = 10$, whose velocity fields were shown in figures 16 and 17. In figure 18(*a–c*), we show the r-component of the

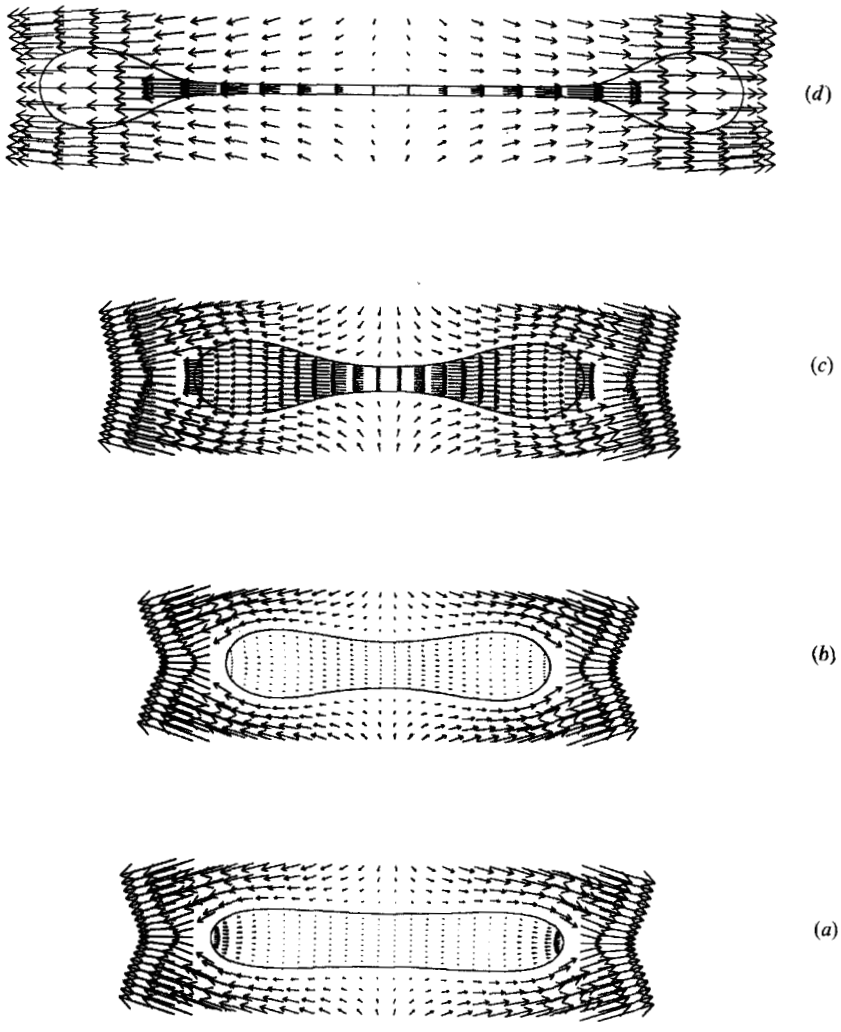

FIGURE 17. As figure 16 but for $\lambda = 10.0$. The simulations correspond to the intermediate shapes shown along curve B in figure 15.

interfacial velocity field as a function of axial position and in figure 18(*d–f*) we show the z-component. In these figures the solid line is the 'exact' numerically calculated interfacial velocity, the dotted line is the undisturbed velocity and the long-dashed line is the difference between the actual velocity and the undisturbed velocity. In the case $\lambda = 1$, this difference is attributable to the flow produced by interfacial tension as a consequence of curvature variations along the surface (see (4)). For $\lambda = 10$, the interpretation is more complex, as we can see from (4).

In figure 18(*a*) the decomposition is shown just after the step reduction in shear rate occurs and in figure 18(*b*, *c*) the results are shown at later times. Relaxational flows are characterized by $u_z < 0$ and the pinching process is produced by $u_r < 0$. The first feature to notice is that, at first (i.e. figure 18*a*) the flow produced by interfacial tension (the long-dashed line) opposes the thinning of the cylindrical midsection. This is evident from the fact that the interfacial-driven contribution to the radial velocity component near the centre of the drop field is positive, and the contribution to the axial velocity field is negative, corresponding to flow towards the centre.

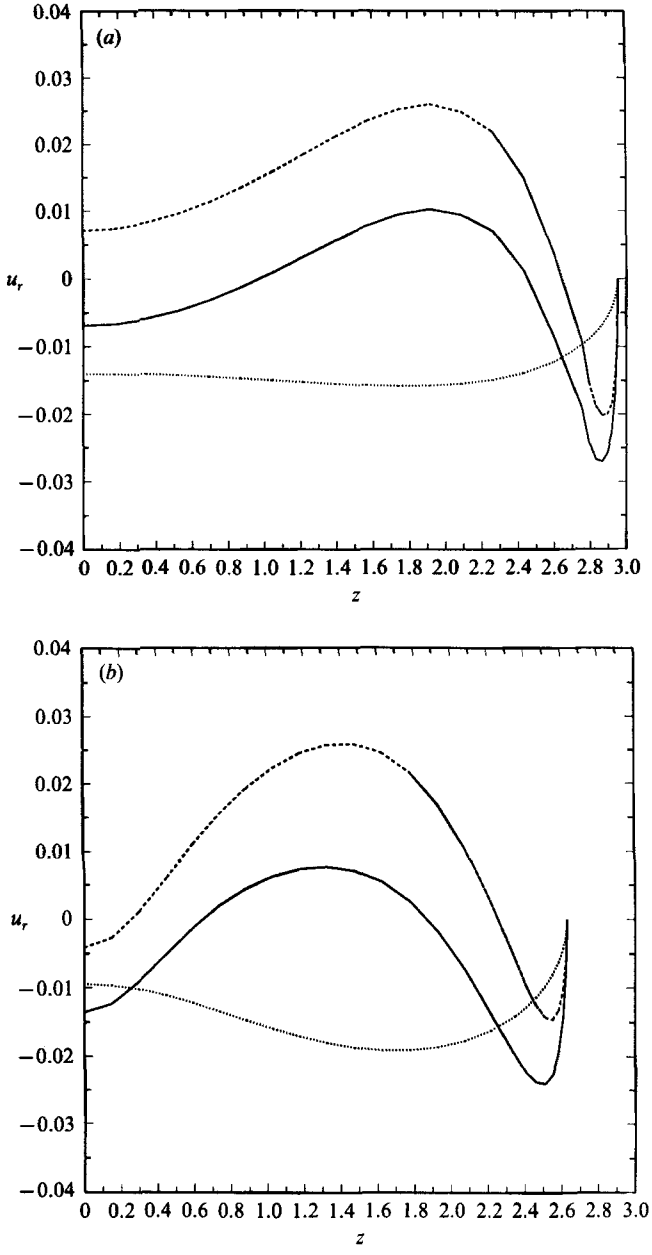

FIGURE 18(*a*, *b*). For caption see page 257.

The later stages of the breakup process are examined in figure 18(*b*, *c*). As the middle region thins the resistance to stretching, due to the interfacial-tension-driven flow, diminishes. In figure 18(*c*), where the midsection is thin, a cooperative flow is produced where both the external flow and the interfacial-tension-driven flow (which only depends on the instantaneous drop shape and λ) result in fluid draining from the centre. This is illustrated by the negative values of u_r and positive values of u_z near the middle of the drop. In figure 18(*b*) the contribution of interfacial-tension-driven flow to the thinning of the drop midsection ($u_r < 0$) is small, while at the later time

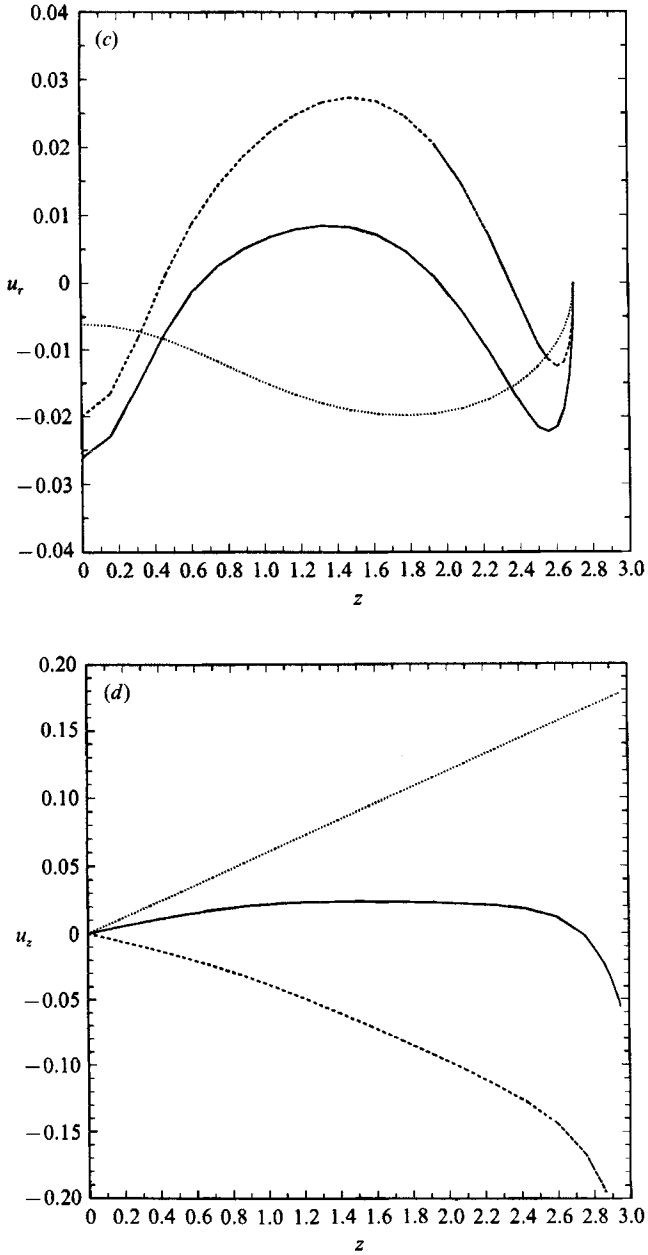

FIGURE 18(*c*, *d*). For caption see facing page.

shown in figure 18(*c*) the rapid pinching is predominately due to the interfacial-tension-driven flow. The evolution of the velocity field shown in figure 19 for $\lambda = 10$ is similar. The main difference for this high viscosity ratio is that the internal velocity gradients are damped significantly. As a result, the radial velocity field that produces thinning of the midsection is weaker than in the $\lambda = 1$ case, and it takes longer for the interfacial-tension-driven flow to dominate and produce the end-pinching effect.

It is important to point out that the undisturbed flow field alone does not produce complete fracturing. Rather, the extensional undisturbed velocity field results in a

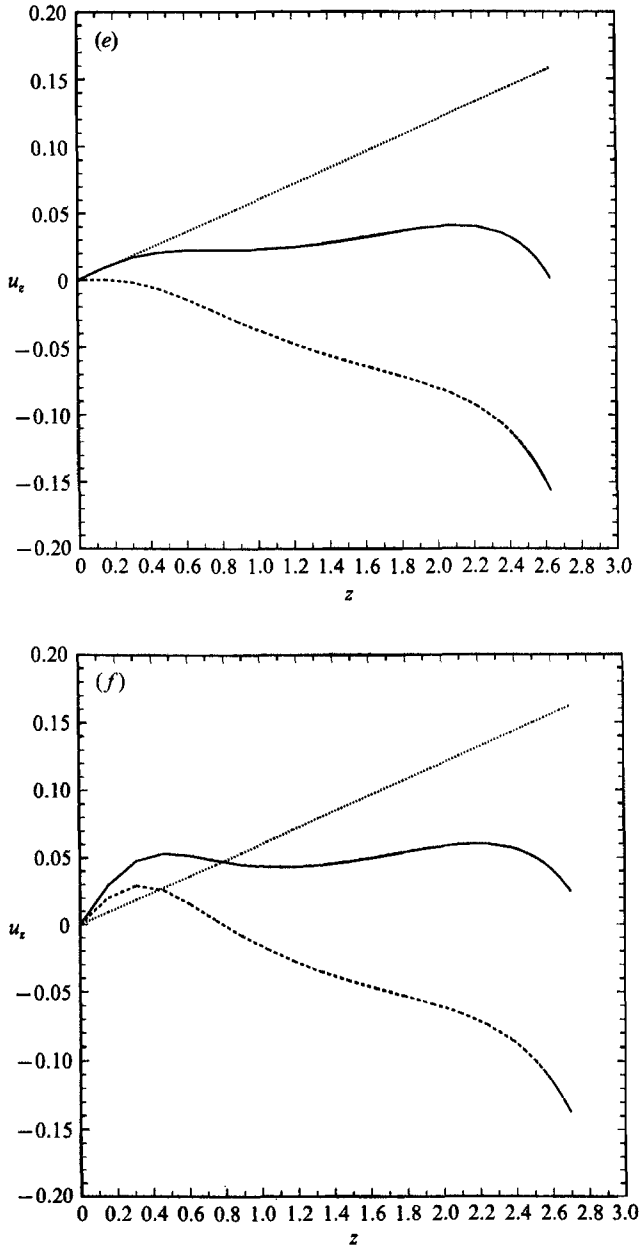

FIGURE 18. The contribution of an interfacial-tension-driven flow to the drop breakup process; the volution of the velocity field. ——, numerically calculated interfacial velocity as a function of axial position; · · · · · ·, contribution of the external flow; - - - - -, difference between the actual velocity and the external velocity. $\lambda = 1.0$. (*a–c*) u_r *vs.* z; (*d–f*) u_z *vs.* z.

simple stretching of the droplet and, as discussed by Mikami *et al.* (1975) for the special case of an infinite, uniform-radius cylindrical thread, such a flow uniformly thins the cylindrical body of fluid. The fracturing process is a direct consequence of the non-uniform flow produced by curvature variations along the drop surface. It is also clear, though, that the weak external flow is necessary initially to cause thinning

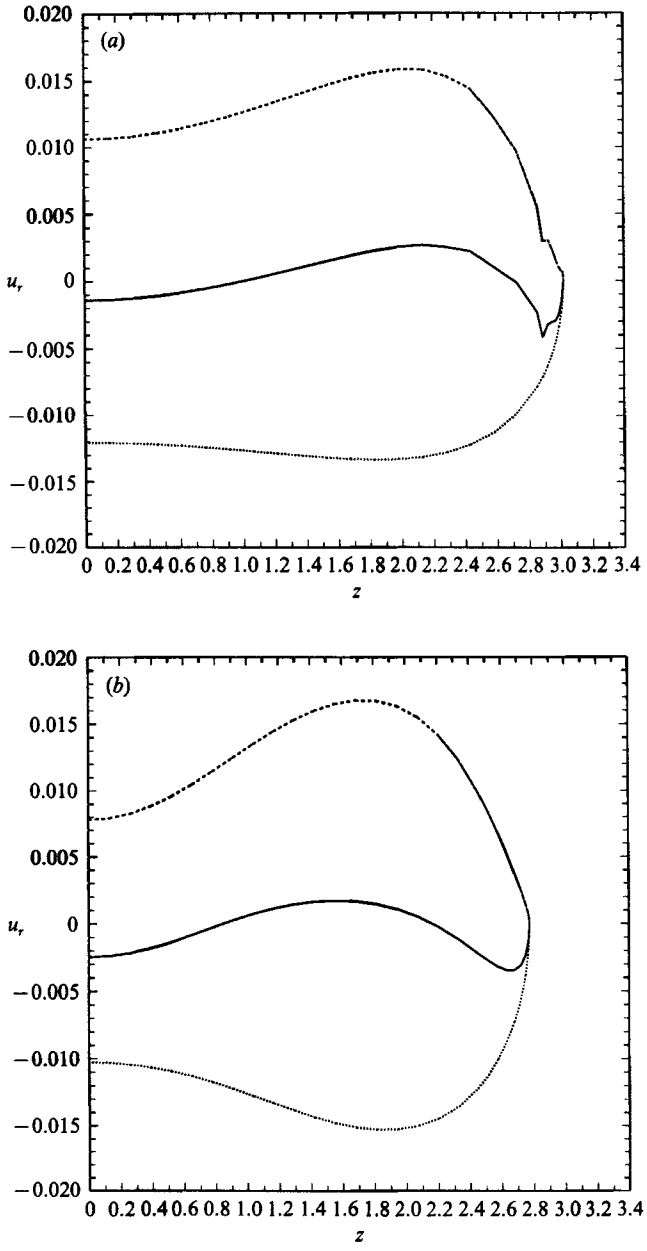

FIGURE 19(*a*, *b*). For caption see page 260.

of the drop midsection until the interfacial-tension-driven flow takes over and produces breakup.

8.4. *Varying the step reduction in G for a given initial shape*

In the preceding sections, we have focused primarily on variations of the initial degree of drop extension for fixed flow conditions. A second aspect of the transient dynamics that we wish to study is the effect of the magnitude of the shear rate reduction for a given initial drop shape. In figures 20 and 21 we illustrate the dynamics

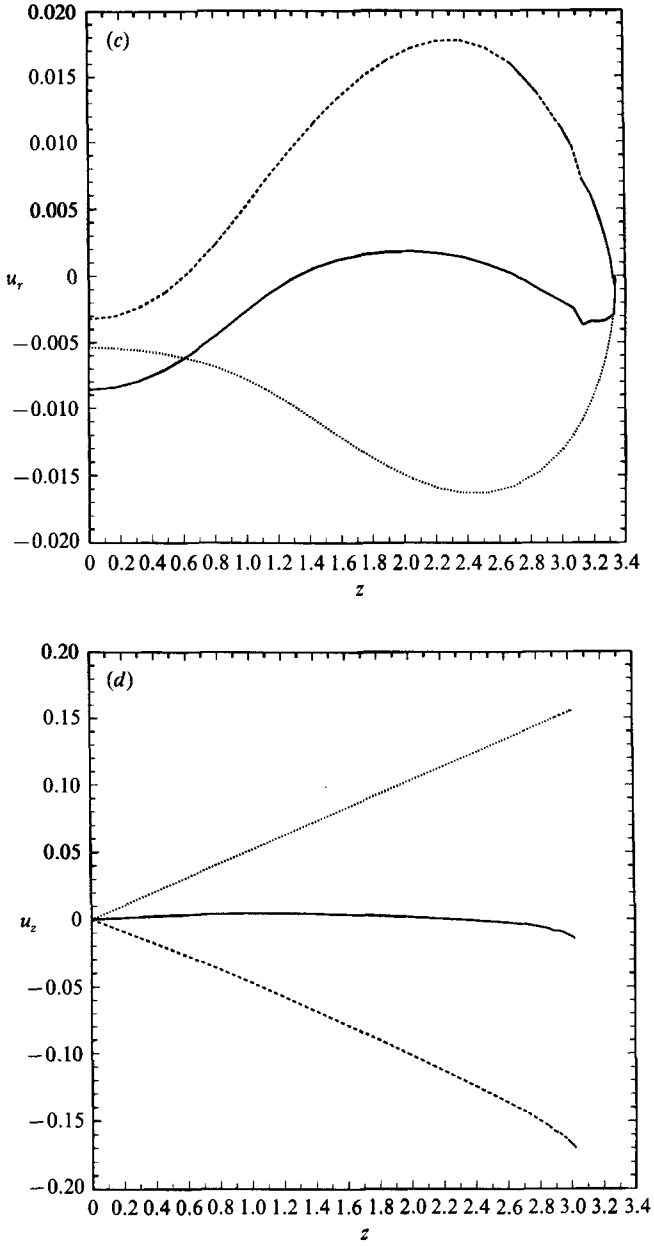

FIGURE 19(*c*, *d*). For caption see facing page.

of a series of drops with $\lambda = 1.0$ and 10 and a fixed initial elongation $L/a \approx 3$, for step changes in capillary number ranging from $\mathbb{C}_c$ to $\beta\mathbb{C}_c$ where $0.25 \leqslant \beta \leqslant 1.0$. In every case where the drop relaxes back to a steady, ellipsoidal shape it does so monotonically and we find numerically that it is the same steady shape as would be generated if an initially spherical drop were placed in the same subcritical flow conditions. This is reported in the inset to these figures where the deformation parameter D† is compared for the case of a spherical drop placed in the flow $\mathbb{C} = \beta\mathbb{C}_c$

† $D = (L-B)/(L+B)$ where L and B are the half-length and half-breadth of the drop.

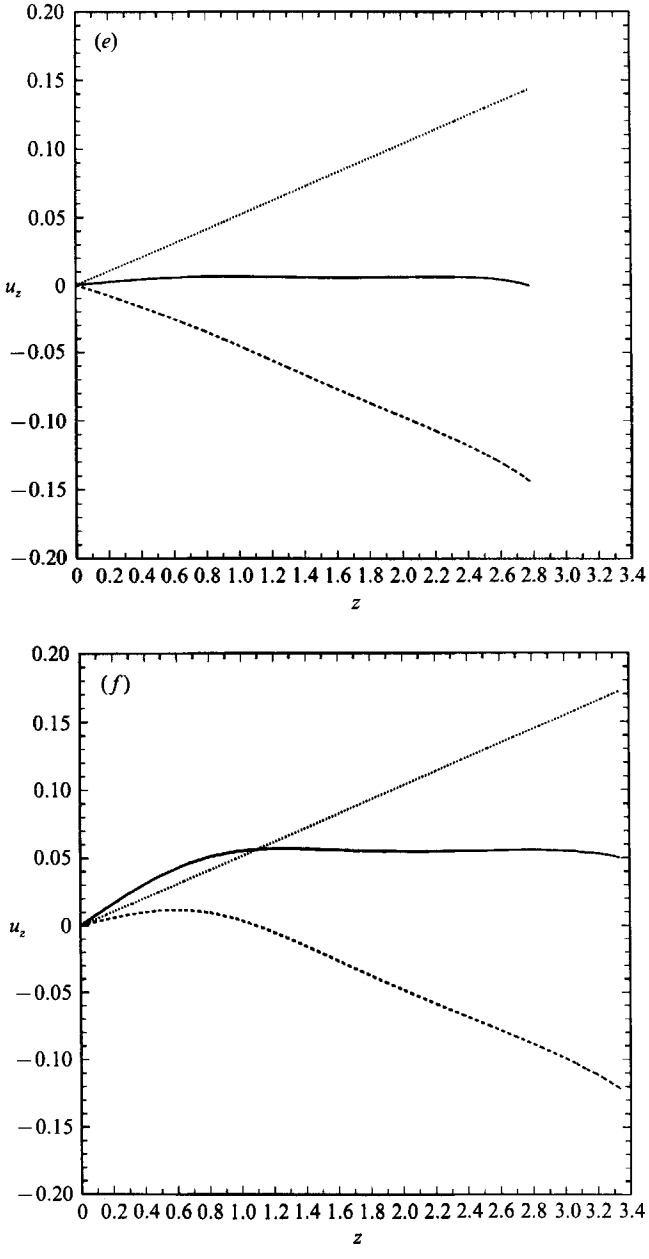

FIGURE 19. As figure 18 but with $\lambda = 10$.

(denoted as D_{ss}) and for the transient approach to the steady state shown in figure 20 and 21 (denoted as D_{trans}).

Clearly, figures 14–21 show that there is a complicated interaction between interfacial-tension-driven relaxation, dependent on the drop shape and the viscosity ratio, and the external extensional motion, which is dependent basically on the capillary number and the initial shape. The numerical results indicate that there is a narrow range of capillary numbers where breakup is preceded by a visible reduction in end-to-end length.

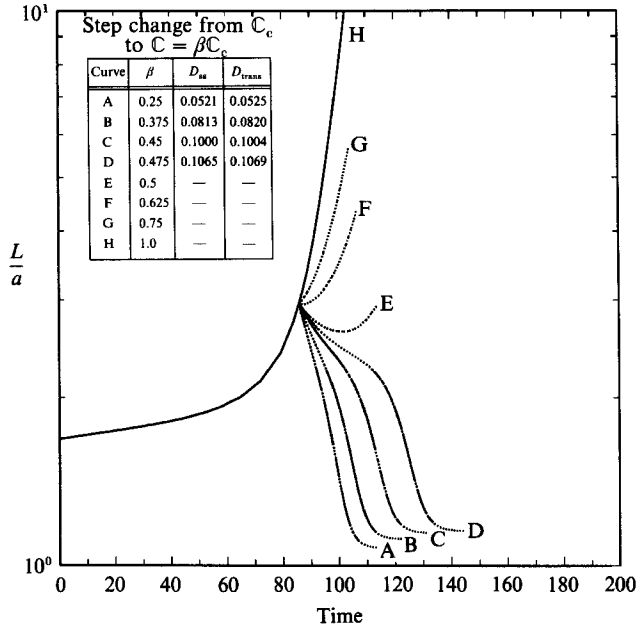

FIGURE 20. Numerical simulation of the effect of changes to subcritical capillary number for a given modestly deformed initial shape. $\lambda = 1.0$.

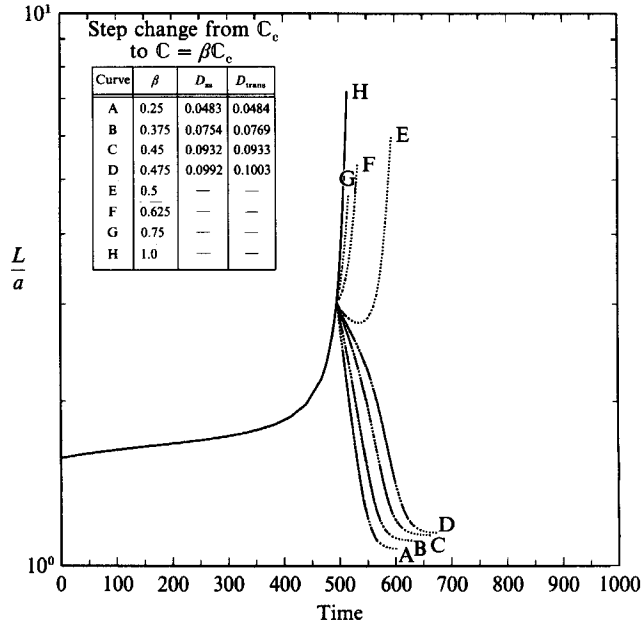

FIGURE 21. As figure 20 but with $\lambda = 10.0$.

9. Conclusions

In this paper we have presented an experimental and numerical investigation of the effect of subcritical flows, produced by step changes in shear rate or flow type, on the breakup of drops stretched initially beyond their maximum steady deformation. The concept of an effective capillary number, based on the new flow conditions, has proven useful for describing necessary conditions for breakup and this is even true in situations where the drop is caused to rotate due to the sudden addition of vorticity. The boundary-integral method is used to visualize the velocity fields during the shape evolution, and clearly illustrates the influence of the external motion and the relaxational interfacial-tension-driven motion on the breakup process.

This work was supported by a grant from the fluid mechanics program of the National Science Foundation. One of the authors (H.A.S.) was partially supported through an IBM Graduate Research Fellowship. We wish to thank one of the referees for several helpful suggestions.

REFERENCES

Acrivos, A. 1983 The breakup of small drops and bubbles in shear flows. *Ann. N.Y. Acad. Sci.* **404**, 1–11.

Acrivos, A. & Lo, T. S. 1978 Deformation and breakup of a slender drop in an extensional flow. *J. Fluid Mech.* **86**, 641–672.

Bentley, B. J. & Leal, L. G. 1986*a* A computer-controlled four-roll mill for investigations of particle and drop dynamics in two-dimensional linear shear flows. *J. Fluid Mech.* **167**, 219–240.

Bentley, B. J. & Leal, L. G. 1986*b* An experimental investigation of drop deformation and breakup in steady two-dimensional linear flows. *J. Fluid Mech.* **167**, 241–283.

Goedde, E. F. & Yuen, M. C. 1970 Experiments on liquid jet instability. *J. Fluid Mech.* **40**, 495–511.

Grace, H. P. 1971 Dispersion phenomena in high viscosity immiscible fluid systems and application of static mixers as dispersion devices in such systems. *Engng Found. Res. Conf. Mixing, 3rd, Andover, N.H.* (Republished 1982 in *Chem. Engng Commun.* **14**, 225–277.)

Kang, I. S. & Leal, L. G. 1987 Numerical solution of axisymmetric, unsteady free-boundary problems at finite Reynolds number I. Finite-difference scheme and its application to the deformation of a bubble in a uniaxial straining flow. *Phys Fluids* **7**, 1929–1940.

Lasheras, J. C., Fernandez-Pello, A. C. & Dryer, F. L. 1979 Initial observations on the free droplet combustion characteristics of water-in-fuel emulsions. *Combust. Sci. Tech.* **21**, 1–14.

Mikami, T., Cox, R. G. & Mason, S. G. 1975 Breakup of extending liquid threads. *Intl J. Multiphase Flow* **2**, 113–138.

Peregrine, D. H. 1986 The dripping of drops, or the bifurcation of liquid bridges. *IUTAM Symposium: Fluid Mechanics in the Spirit of G. I. Taylor, Symposium Abstracts.*

Rallison, J. M. 1984 The deformation of small viscous drops and bubbles in shear flows. *Ann. Rev. Fluid Mech.* **16**, 45–66.

Rallison, J. M. & Acrivos, A. 1978 A numerical study of the deformation and burst of a viscous drop in general shear flows. *J. Fluid Mech.* **89**, 191–200.

Seward, T. P. 1974 Elongation and spheriodization of phase-separated particles in glass. *J. Non-Cryst. Solids* **15**, 487–504.

Sherwood, J. D., 1988 Breakup of fluid droplets in electric and magnetic fields. *J. Fluid Mech.* **188**, 133–146.

Stone, H. A. 1988 Dynamics of drop deformation and breakup in time-dependent flows at low Reynolds numbers. Ph.D. thesis. California Institute of Technology.

Stone, H. A., Bentley, H. J. & Leal, L. G. 1986 An experimental study of transient effects in the breakup of viscous drops. *J. Fluid Mech.* **173**, 131–158.

STONE, H. A. & LEAL, L. G. 1989 Relaxation and breakup of an initially extended drop in an otherwise quiescent fluid. *J. Fluid Mech.* **198**, 399–427.

TAYLOR, G. I. 1932 The viscosity of a fluid containing small drops of another fluid. *Proc. R. Soc. Lond.* A **138**, 41–48.

TAYLOR, G. I. 1934 The formation of emulsions in definable fields of flow. *Proc. R. Soc. Lond.* A **146**, 501–523.

TORZA, S., COX, R. G. & MASON, S. G. 1971 Electrohydrodynamic deformation and burst of liquid drops. *Phil. Trans. R. Soc. Lond.* A **269**, 295–319.

TORZA, S., COX, R. G. & MASON, S. G. 1972 Particle motions in sheared suspensions. 27. Transient and steady deformation and burst of liquid drops. *J. Colloid Interface Sci.* **38**, 395–411.

VAN DYKE, M. 1982 *An Album of Fluid Motion*, p. 73. Parabolic.